NTNU
Norwegian University of
Science and Technology

Black Silicon Structures

Maren Elise Juul

Materials Science and Engineering (MTMT)
Submission date: January 2018
Supervisor: Ingeborg Kaus, IMA

Norwegian University of Science and Technology
Department of Materials Science and Engineering

Abstract

Nanostructuring on the surface of silicon can make high efficient solar cells possible by lowering the reflection. Silicon wafers were successfully wet chemically etched with metal-assistance, to create a black silicon structure (BSiS). Different passivation layers and methods, PECVD and chemical, were tested with the purpose of decrease surface recombination. Silicon oxide was applied with PECVD with four different deposition times; 15, 30, 45 and 60 seconds. All the samples had promising surface structure and low reflection, ≤1%. The samples with shortest (15s) and longest (60s) deposition time had the most promising cross-section structures. However, the intermediate times (30s and 45s) were assumed to have been destroyed when preparation for the cross-section images, making these results misleading. A passivation layer of silicon nitride was deposited with PECVD with four different deposition times; 60, 120, 180 and 240 seconds. The samples with the shortest deposition times (60s and 120s) kept the same low reflection, below 2%, and BSiS after deposition.

A passivation layer of alumina was successfully deposited chemically by dip coating and annealing of the wafer at 600°C for 3 hours. Ag plasmonic nanoparticles were mixed into the alumina solution and passivated with the same chemical production steps as the alumina passivation layer without Ag nanoparticles. The Ag nanoparticles was observed and verified with TEM. Low reflection, less than 1%, and the BSiS was kept after deposition of the passivation layer, both with and without Ag nanoparticles.

Sammendrag

Nanoteknologi på overflaten til silisium kan gjøre det mulig å produsere solceller med høy effektivitet ved å senke refleksjonen. Wafere ble vellykket våtkjemisk etset med metal-assistanse, for å skape en sort silisiumstruktur(BSiS). Ulike passiveringsbelegg og deponeringsmetoder, PECVD og kjemisk, ble testet. Silisiumoksid ble påført med PECVD med fire ulike deponeringstider; 15, 30, 45 og 60 sekunder. Alle prøvene hadde en lovende overflatestruktur og lav refleksjon, ≤1%. Prøvene med kortest (15s) og lengst (60s) deponeringstid hadde den mest lovende tverrsnittsstrukturen. De midterste tidene (30 og 45s) antas å ha blitt ødelagt ved preparing for tverrsnittsavbildning, hvilket gjør disse resultatene misvisende. Et passiveringsbelegg av silisiumnitrid ble deponert med PECVD med fire ulike deponeringstider; 60, 120, 180 og 240 sekunder. Prøvene med de korteste deponeringstidene (60 og 120s) har beholdt den samme lave refleksjonen, under 2%, og BSiS etter deponering.

Et passiveringsbelegg av alumina ble vellykket deponert kjemisk på en prøve med BSiS ved å legge dypp-belegg og gløde waferen ved 600ºC i 3 timer. Ag plasmoniske nanopartikler ble blandet inn i alumina-løsningen og passivert med de samme kjemiske produksjonsstegene som beskrevet over. Ag nanopartikler ble observert og bekreftet med TEM. Lav refleksjon, under 1%, og BSiS var vedvart etter deponering av passiveringsbelegget, både med og uten Ag nanopartikler.

Preface

This report is the result of a master's thesis done at the Department of Material Science and Engineering at the Norwegian University of Science and Technology (NTNU). The master project has been carried out fall 2017, as a part of my education within a Master of Science degree in Material Science and Engineering. The aim of this thesis was to investigate possible passivation methods and materials for black silicon structures and possible incorporation of silver plasmon nanoparticles. This work is a direct sequel of the specialization project carried out by the undersigned during the fall of 2016.

Endless gratitude towards Ingeborg Kaus, who has given me guidance and support through the whole process.

Big thanks to Jannicke Kvello who gave med all the laboratory training. Thanks to Arne Røyset for helping with the optical characterization and guidance within plasmonic nanoparticles. I will give a thanks to Sidsel Meli Hanetho for helping with deposition of the plasmon nanoparticles. Thanks to Ragnhild Sæterli and Bjørn Gunnar Soleim for helping me prepare the sample and execute characterization with TEM. The TEM work was carried out using NORTEM infrastructure, Grant 197405, TEM Gemini Centre, Norwegian University of Science and Technology (NTNU), Norway. Thanks to Gaute Stokkan for helping with recombination measurements. Finally, I would like to thank Benedikte Jørgensen Myrold for keeping me company for my last semester at NTNU and Jan Inge Hammer Meling who always keeps me well fed.

Trondheim, January 2018

Maren Elise Juul

Table of Content

1 Introduction

Solar power is an endless power source, available all over the world. Solar cells are maybe one of the most well-known ways of collecting the power. The main goal of solar cell research is to create solar cells with high efficiency and lowered production costs. If the electricity generated by solar cells is as cheap or cheaper than the electricity that is purchased from the electrical grid, then solar energy has reached grid parity. The industry is producing thinner wafers to lower the production costs, but this causes new problems that decrease the solar cell efficiency. Black silicon structures have a porous nanostructure on the surface that decreases the reflection, with the intention of increasing the efficiency.

There are different ways to create the black silicon solar cells, e.g. electrochemical etching, stain etching, metal-assisted chemical etching or reactive ion etching[1]. Metal-assisted chemical etching is a simple production method that has shown promising results. There are several parameters that can be varied. This has been investigated in a specialization project, fall 2016[2]. All samples with black silicon structure had decreased reflection compared to an untreated crystalline silicon wafer. The samples etched in an ice bath for 20 min had the most promising optical properties with less than 1% reflection within the visible part of the solar spectrum. These samples are used as a basis for the research done in this master thesis.

The black silicon structure is a nanostructure on the surface that increases the surface area. The low reflection gives a promising future for black silicon structures for the solar cell industry, but there are some challenges to overcome before it is ready for the industrial market. Combining thinner wafers and increased surface area, the surface recombination is increased, and the cell efficiency decreased. Recombination can be reduced by reducing the density of surface states or by reducing the concentration of free electrons or holes at the surface[3]. A passivation layer is one possible solution for reducing recombination. It can be deposited with different methods, e.g. ALD, PECVD or chemically, and can consist of different materials. It can be a single layer or a combination of several different materials in a multi-layer structure. The efficiency of the solar cell is highly dependent on the thickness of the passivation layer. A thick layer can damage the optical effect, but it must be thick enough to get the effect of a surface passivation layer.

A good passivation layer on the black silicon structure can increase the efficiency of a solar cell, compared to an untreated planar crystalline solar cell, but it might be possible for even higher efficiency. Plasmonic effect has earlier been used and researched especially within thin

film solar cells, because the narrow film layer gives restriction regarding surface texturing[4]. Plasmonic nanoparticles from a noble metal can create surface plasmon resonance at the surface, when exposed to light. Silver and gold have earlier been the preferable materials for the plasmonic nanoparticle[5]. Light trapping may be increased if the scattering from the nanoparticle is near the localized plasmon resonance, hence increased efficiency of a solar cell. The nanoparticles should have a uniform and homogenous distribution on the surface and their size and shape must be controlled to get the desired effect[5]. This master thesis investigates the possibility of including silver nanoparticles within an alumina passivation layer, on the black silicon structure, with the hopes of a plasmonic effect and with that, increase the efficiency further. Grid parity could be possible, if the great optical properties of the black silicon structure is intact after deposition of the passivation layer with or without the plasmonic nanoparticles.

2 Theory

The project is based on the use of black silicon structures, created by metal-assisted wet chemical etching. Further theory on the subject and production method has been explained in the previous specialization project[2]. In the project, different etching times and temperatures were examined. The results showed that the samples that were etched in an ice bath for 20 min, gave the lowest reflection. These parameters are hence used as the basis for this master thesis. The samples etched in ice bath for 20 min have a porous needle-like nanostructure, approximately 7-8µm thick. Shorter nanostructures decrease the recombination and absorption[6].

A passivation layer is used both as an anti-reflection coating (ARC) and to lower the recombination of conventional crystalline silicon. Because the black silicon structure sample has only 1% reflection, the following passivation layers will not be evaluated with regards for the ARC properties. The black silicon structure work as a textured antireflection solution. This makes it possible to combine two production processes, texturing and ARC, into one step and therefore possibly reduce the production costs. Since there are not the same requirement for ARC, thinner passivation layers on BSiS solar cells may be possible.

Plasmonic nanoparticles have previously been investigated as an increasing efficiency effect for thin film solar cells[4, 7]. The nanoparticles were found to elongate the light path within the solar cell, thus increasing its efficiency. This thesis aims to incorporate the plasmonic nanoparticles within the passivation layer. This would make it possible to increase the efficiency even further, without adding any production steps. The plasmonic nanoparticles could improve the optical properties for solar cells in addition to the black silicon structures.

2.1 Optical properties

The optical properties of a semiconductor can be divided into four categories; refraction, reflection, absorbance and transmission. The light that is not absorbed or reflected, gets transmitted through the medium.

When light travels through a medium the refractive index, n, can give an indication on how it travels through the medium. Light will experience a change in velocity and therefore bend at the interface of the medium. In Equation 1, n is a dimensionless value, calculated by dividing the speed of light, c, on the velocity of light in the material, v.

$$n = \frac{c}{v} \tag{1}$$

The antireflection or dielectric layer should have a refractive index between that of crystalline silicon and free space. The black silicon structure should have the same refractive properties as an antireflection layer, since there are no antireflection coatings. Silicon has a high refractive index, approximately 3.4 within visible light[8], meaning that it is highly reflective. Because the black silicon structure has a non-uniform interface, the refractive index will be varying within the structure as well as for the wavelength. The refractive index will increase from the top of the structure (air) to the bottom of the nanostructure(silicon). The black silicon structure in-between will have created a step change in the refractive index, if there is a constant porosity in the nanostructure. If the nanostructure has a graded porosity, the refractive index can have a smooth transition from air to the substrate silicon.

The dielectric constant, ϵ_r, can be calculated from the refractive index. The dielectric constant, ϵ_r, can be used for defining the refractive index in Equation 2, where μ_r is the relative magnetic permeability[9]:

$$n = \frac{c}{v} = \frac{\sqrt{\epsilon\mu}}{\sqrt{\epsilon_0\mu_0}} = \sqrt{\epsilon_r\mu_r} \tag{2}$$

These constants can be useful when explaining the function of the plasmonic nanoparticles.

When an electron gets excited by a photon, an electron-hole pair is established as mobile charge carriers. This process occurs when light gets absorbed and is called generation. The opposite mechanism is called recombination. Some of the light will be reflected at the interface, which is calculated by dividing the reflected beam on the incident light. A high index of refraction gives high reflection. The amount of reflection is dependent on the wavelength of the incoming light. Solar cells should have close to zero reflection to obtain maximum efficiency. A big step towards this goal is by using black silicon structures on the surface of wafers in solar cell panels.

2.2 Recombination

Generated electrons will try to fall back to its original position because of thermal equilibrium, which arises recombination. The charge carrier may be “delayed” before arriving at its original position. This results in recombination losses, both in the bulk and at the surface, via defects levels and/or due to dangling bonds, within the bandgap. Silicon has an indirect bandgap, so that the electrons need a change in momentum as well as an energy change. This extra factor can cause more delays for the electrons and hence more recombination losses.

2.2.1 Dangling bonds

Covalent bonding connects silicon atoms in a diamond structure throughout the bulk of silicon. The crystal orientation determines if there are one or two non-saturated or "dangling" bonds at the surface. This project will use silicon with (100) orientation, resulting in two available bonds at the surface[10]. The second layer of bonds is referred to as the backbonds, as illustrated in Figure 2.1.

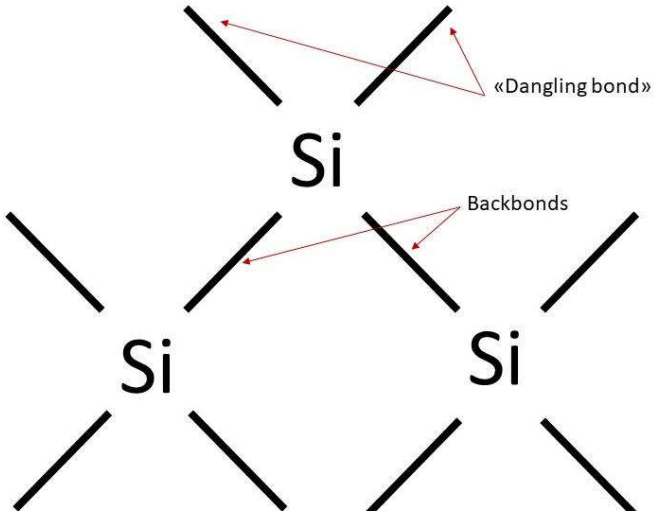

Figure 2.1. Silicon diamond structure surface (100). Illustrates the available or "dangling" bonds at the surface and the backbonds as the second layer.

The dangling bonds cause a large density of defects, intrinsic or extrinsic, within the bandgap at the surface. Extrinsic defects, i.e. dislocations or chemical residues, are highly disposed to different recombination mechanisms.

2.2.2 Recombination mechanisms

There are three different types of recombination; radiative, Auger and Shockley-Read-Hall (SRH). Radiative recombination is spontaneous emission[8]. It is unavoidable and negligible for indirect semiconductors, compared to the other two, and will not be further addressed in this thesis.

Auger recombination involves three charge carriers. An electron recombines with a hole and the excess energy goes to exciting a third charge carrier high into the conduction band. The Auger recombination is dependent on the doping level. High doping level gives short Auger lifetime. There are two different equations for the lifetime of Auger, one for the p-type doped materials, 3*a,* and one for n-type doped materials, 3*b*[8].

$$\tau_n = \frac{1}{A_n N_a^2} \tag{3a}$$

$$\tau_p = \frac{1}{A_p N_d^2} \tag{3b}$$

A_n and A_p is the Auger coefficients and N_d is the concentration of donor atoms and N_a is the concentration of acceptor atoms. Auger recombination is a problem for semiconductors with indirect bandgap, like silicon. Auger recombination may be higher for black silicon structure, since the structure gives the surface a heavier and non-uniform doping.

SRH recombination happens when the charge carrier recombines via an extra energy level, within the forbidden bandgap. Since silicon has an indirect bandgap, the SRH recombination will be dominating. This type of recombination is dependent on defects, impurities, etc., all of which are at a high concentration at the surface. The SRH lifetime is defined by Equation 4, where *a* or *b* depends on whether the wafer is a n- or p-type wafer[8]:

$$\tau_{n,SRH} = \frac{1}{B_n N_t} \tag{4a}$$

$$\tau_{p,SRH} = \frac{1}{B_p N_t} \tag{4b}$$

Here, B_n and B_p are the coefficient defined in Equations 5*a* and 5*b*, and N_t the density of trap states at an energy E_t in the band gap.

$$B_n = v_n \sigma_n \tag{5a}$$

$$B_p = v_p \sigma_p \tag{5b}$$

v_n is the mean thermal velocity of the electron that is captured in an empty trap, from the conduction band. The capture cross section of the trap for the electron is defined as σ_n. The same values are defined with p, instead of n, for the holes that are captured from the valence band. SRH recombination can be simplified for doped semiconductors and expressed with the lifetime. Equation 6*a* is for the n-type materials and 6*b* for p-type materials[8].

$$U_{SRH} \approx \frac{(p - p_0)}{\tau_{p,SRH}} \tag{6a}$$

$$U_{SRH} \approx \frac{(n - n_0)}{\tau_{n,SRH}} \tag{6b}$$

The equations show that a low lifetime for the material, will give a high recombination, U_{SRH}.

The total lifetime is calculated by adding the lifetime of the three different recombination mechanisms. A short lifetime indicates high recombination losses. The minority carriers

determine the lifetime and is therefore used for the calculations. Carrier recombination lifetime, Equation 7[3]:

$$\tau \equiv \frac{\Delta n}{U} \tag{7}$$

U is the net recombination rate and Δn are the excess minority carrier concentration, corresponding to $\Delta n \equiv n - n_0$ and $\Delta p \equiv p - p_0$. n/p is the electron/hole concentration and n_0/p_0 is the thermal equilibrium concentrations of electrons/holes. In an ideal situation, the same number of electrons and holes will be generated and then the excess concentrations of electrons and holes will be equal, $\Delta n = \Delta p$.

Because of the dangling bonds and a large density of defects at the surface, there is an unbalance within the symmetry of the crystal lattice. Since black silicon structures creates a needle-like surface, the surface area is increased, and therefore increasing the surface recombination. Recombination can be reduced by reducing the density of surface states or by reducing the concentration of free electrons or holes at the surface[3]. The density of surface states can be reduced with application of a passivation layer. The concentration of free electrons or holes at the surface can be reduced by the formation of an internal electric field below the semiconductor surface. This is due to electrons and holes carrying electrical charge that causes the concentration of one carrier (hole or electron) to be reduced. This electrical-field effect can also be created from a passivation layer.

2.3 Passivation layer

There are different methods and different materials that are suitable for passivation of the surface. A passivation layer has the purpose of reducing the recombination. It should be thermal and chemical stable, homogenous distributed and produced inexpensively. The passivation layer can contain one material in a single layer or combine different materials in a multi-layer. Two materials in a double layer makes it possible to combine the properties from the two different materials.

There are two types of passivation layers. The chemical, which reduces the surface defect states (dangling bonds). The other is field-effect passivation, which shields minority charge carriers from the surface. The highest recombination rate is when the hole and electron densities at the surface are approximately equal. A field-effect passivation layer has an electric field at the surface that reduces the density of one of the charge carriers (either holes or electrons). If the holes are shielded at the interface, the passivation layer has a positive

charge density. Both passivation layers would reduce the recombination and increase the efficiency of a solar cell.

The key to a good passivation layer is to find the optimal thickness. It should be as thin as possible to not damage the optical effect, but also thick enough to get the desired effect of a surface passivation layer. Because of the nanostructure on the surface, the deposition time and deposition rate will have to be considered. The passivation layer needs to be deposited in all the pits in the black silicon structure, so that the whole surface is covered, and all the dangling bonds are saturated. A thick passivation layer may fill some of the pits, resulting in not getting the desired optical effect from the nanostructure. The goal is to have a homogeneous layer, with uniform thickness throughout the black silicon structure.

Different methods have showed promising results, e.g. ALD, PECVD, PVD, CVD, electrochemical, wet chemical or thermal for deposition of a passivation layer[11-18]. ALD (atomic layer deposition) is one of the most promising methods because of the conformality to nanostructured surfaces and good thickness control[1, 11, 19], but it requires equipment that was not available during this thesis. ALD is a complicated and expensive method and it would be preferable to find other production options. Plasma Enhanced Chemical Vapor Deposition (PECVD) have the advantage of already being used on planar crystalline silicon in the solar industry. This is helpful since the method is expensive, and it would be preferable if not all new equipment had to be purchased. PECVD makes it possible to deposit at low temperatures. Thermal oxide can give a passivation layer that reduces the interfacial defects and a small amount of positive fixed charge, giving a weak field-effect passivation layer. The main disadvantage is the high process temperature, which can be problematic because of for instance increased impurities. Another low temperature method is wet chemically deposition, which is cheap and easy to reproduce at an industrial scale. The disadvantage is the reduced control of uniformity, thickness and conformality.

2.3.1 PECVD

PECVD gives the possibility to deposit thin films at low temperatures. This is a great advantage, regarding carrier lifetime degradation, dopant redistribution and cleanliness requirement, among other factors[3]. When depositing with direct PECVD, the samples are located within the plasma and all the gases are excited by an electromagnetic field. A major disadvantage with the method, is that it is expensive and complicated. A cheaper alternative is the remote PECVD. This method uses a spatially separated excitation of the plasma from the sample. There are different possible plasma excitation approaches, e.g. microwaves, hollow

cathode or arc jet[17]. Remote PECVD will also be more suitable for black silicon structures, since the wet chemical etching creates nanostructures on both sides of the wafers, making it difficult obtaining the required electrical contact between wafer and wafer-holder in direct PECVD. Non-electrical contact also makes thinner wafers possible. Keeping that in mind, there is only direct PECVD available through this project and will therefore be used for this research.

2.3.1.1 Silicon oxide

Silica reduces the silicon interfacial defects and contributes with a fixed positive charge, creating an excellent chemical passivation layer and gives a weak field passivation effect. The best results have been showed using a thermal SiO_2, but that requires high temperatures during deposition[1]. This can be problematic, since impurities can diffuse from the grain boundaries into the substrate. A possible alternative is to deposit SiO_x with PECVD, which can be done at much lower temperatures. A passivation layer of silicon oxide can be created by mixing SiH_4, N_2O and N_2, when using PECVD. SiO_x have showed poorer quality in the passivation than SiO_2, but it could be improved by capping Al_2O_3 or a-SiN_y layers[1, 11].

2.3.1.2 Silicon nitride

A material that may be used with the PECVD method is silicon nitride. SiN_y deposited with direct PECVD with high frequency, results in better UV stability and better surface passivation, compared to deposition with low frequency. The layer is easily applied with PECVD, where the SiN_y is created of a mixture of ammonia, silane and nitrogen gas. The plasma gas creates a large amount of hydrogen dissociation and is incorporated in the film. SiN_y is both chemically and thermally stable. There are three parameters that can vary and effect the final passivation film; the gas flow ratio, deposition temperature and deposition time.

Liu et al. have investigated the different effects by variating the parameters[15]. The gas flow ratio between the ammonia and silane gas have a great effect on the film properties. The refractive index increases with decreasing gas flow ratio. This is indicating that an increased Si contain increases the refractive index. The gas flow ratio also influences the density of the film. The Si content will decrease if the gas flow ratio increases, resulting in a denser film due to a slower growth rate. The temperature for passivating SiN_y is around 300-400°C. A high deposition temperature can diffuse hydrogen atoms into the silicon substrate and therefore reduce the recombination center. The high deposition temperature gives high minority carrier lifetime and high conversion efficiency. The final varying parameter is the deposition time. It

is believed that a longer deposition time gives a denser and thicker film. More hydrogen atoms will diffuse into the silicon substrate to passivate defects and dislocations if the deposition time is increased, and therefore resulting in a decreased recombination center. Liu et al found that the ultimate deposition time on black silicon structures is 500 seconds with PECVD of SiN_y[15].

A passivation layer of Si-rich SiN_y would reduce the number of dangling bonds at the surface, acting as chemical passivation. Field-effective passivation is also possible by increasing the nitrogen content and therefore create a high density of fixed positive charges. The positive charges will accumulate a layer near the silicon surface that reduces the minority carrier concentration. One disadvantage of this material choice is that the ending results depends on the doping in the Si. The positive interfacial charge makes it only suitable for n-Si or lightly doped p-Si.

The effect of the layer increases with increasing thickness of the film for a planar crystalline silicon wafer, but is saturated at approximately 20nm[20]. Liu et al. showed that for black silicon structure, a layer thicker than ~20nm had better passivation properties[1, 15]. The disadvantage is that a thick film will increase the serial resistance for printed metal contacts.

2.3.2 Chemical passivation, alumina

Chemical deposition of a passivation layer can be done both electrochemically or wet chemically. Possible materials are silica, alumina or iodine[16, 21, 22]. Production, surface treatment and black silicon structure is still under development and there is no record of chemical passivation of the nanostructure, so far. Alumina have great advantages as passivation layers and have earlier showed promising results[11]. A challenge associated with chemical deposition is the lack of thickness control and it might be problematic to create a uniform and conformal film. The alumina solution can be altered and therefore altering the passivation layer.

A chemical deposition would be preferable, compared to e.g. ALD, since it is a cheaper method. Dip coating is a good example of a chemical deposition method that is possible to use at an industrial scale. The dip coating should be followed by annealing, to decrease the dislocation concentration within the passivation layer. Aluminum oxide, Al_2O_3, is common source for aluminum and it is possible to create an alumina solution (Al sol) by dissolving the powder in e.g. ethanol. A sol-gel deposition gives relatively homogeneous films, carried out at

low temperatures and it is a simple method. The alumina gives great advantages regarding electrical, optical and wear-resistant applications[22].

The passivation layer has an effective field-effect passivation at the Si/Al_2O_3 interface, which shields the electrons from the interface. This is different from the other passivation layers which have positive charge densities and shield the holes from the interface. The alumina oxide creates a negative charge density. Because of the negative fixed charge that induces the field-effective passivation, the material is most suitable for p-type Si. Wafers with high doping densities will reduce the field-effective passivation. Another advantage is that it is transparent and stable under UV illumination.

2.4 Plasmonic effects

Including plasmonic nanoparticles within the passivation layer, can increase the efficiency even further without adding more steps to the production process. By applying plasmonic nanoparticles on the surface, the intention is to scatter light back into the nanostructure. Silver and gold have the desired properties for constructing plasmonic nanoparticles. In a plasmon model, the alkali metals will extend up to the ultraviolet frequency range. Noble metals, on the other hand, will limit the interband transitions to visible frequencies[5].

Metals have a valence electron gas that oscillates back and forth with respect to the ion core. Plasmons are collective oscillations of the quasi-free electrons in metals. This creates a local electromagnetic field, because of the electric charge from electrons. When light strikes the surface, the electric field interacts with the conduction electrons. Light is absorbed at the surface resulting in resonating electron, giving surface plasmon resonance (SPR). The frequency of SPR depends on the nanoparticle material, size, shape, the dielectric properties of the surroundings and inter-nanoparticle coupling interactions[23]. These properties have therefore a great effect on the functionality of the plasmonic nanoparticles.

Light scattering or near-field concentration of light are the two suggested possible mechanisms for the photocurrent enhancement by the metal particle[4]. The particle size, the semiconductor's absorbents and the electrical design of the solar cell determines the contribution of each of the mechanisms. If the wavelength of the incoming light is near the plasmon resonance, could the nanoparticles be strong scatters of light, because of the collective oscillation that the conduction electrons makes. Since the nanoparticles have small surfaces, the possible wavelengths that the surface plasmon can have in a metal, changes. Not all wavelengths are available in a small particle.

Surface plasmon resonance (SPR) occur when the following Equation 8 is met:

$$\varepsilon_p = -2\varepsilon_m \tag{8}$$

Where ε_p is the dielectric function of the plasmon particle and ε_m is the dielectric function of the embedding medium, which corresponds to alumina in this thesis. The scattering cross-section at the SPR can exceed the geometrical cross-section of the nanoparticle. The scattering must be more efficient than the absorption to meet the requirements for good light trapping properties. This can be accomplished with larger particles, e.g. 100nm nanoparticle. For an increasing particle size, the conduction electrons will no longer move in phase, resulting in dynamic depolarization. The depolarization field at the center of the particle will therefore be reduced and the UV spectra show a peak of the absorbance from the plasmon particle. If the nanoparticles are too big (several hundred nanometers) there would be a flatter absorbance, working as bulk material. A surface plasmon will have a lower energy than plasmons in the bulk.

Increased electron density causes an increase in the plasmon resonance frequency. This is showed in the Equation 9 for the plasmon energy.

$$\omega_p^2 = \frac{Ne^2}{m\varepsilon_0} \tag{9}$$

Where ω_p is the plasmon resonance frequency, N is the number density of the electrons, e is the electron charge, m the electron mass and ε_0 is the permittivity of free space. This also proves that the material chosen affects the plasmonic effect.

2.4.1 Ag plasmonic nanoparticles

Noble metals, such as silver, are expensive materials, which is one of the disadvantages of using these metals. Silver nitrate is the cheapest of the silver compounds and was therefore used as a source for possible plasmonic nanoparticles in this project. The main challenge is finding the optimal deposition methods for the nanoparticles. The particles need to have a homogenous distribution on the surface, and the preferable particle size must be taken into consideration.

A suitable method for deposition of silver plasmonic nanoparticles method is chemical deposition. It might be possible to include the plasmon nanoparticles within the passivation layer. This method is favorable because of the simple setup and low production cost. If the chemical passivation layer is a success and it is possible to include the nanoparticles within the layer, the number of production steps would not be increased. This means that there would

be no further production cost for the deposition of the nanoparticles, apart from the cost of the chemicals. This results in high efficient solar cells at a low production cost. Some disadvantages are that there is a minimal control of the shape, size and distribution of the nanoparticles on the surface. A change in concentration of the silver or different production temperatures might affect the particle size.

The plasmon nanoparticles will also influence the optical properties and have an own refractive index. The refractive index of silver is a dispersion, it changes with λ. Because of the variation in *n*, the formula will have an imaginary and a real part, giving a complex refractive index, Equation 10[5].

$$\tilde{n}(\omega) = n(\omega) + i\kappa(\omega) \tag{10}$$

The function is of angular frequency ω, ñ = √ε and κ is the extinction coefficient, which determines the optical absorption of electromagnetic waves propagating through the medium.

3 Experimental

The black silicon structure was created with metal-assisted wet chemical etching[2]. Silicon wafers were etched in an ice bath for 20 min. One sample was kept as reference for comparison. The samples with the black silicon structure were applied with different passivation layers, with different methods. The different production routes are illustrated in Figure 3.1.

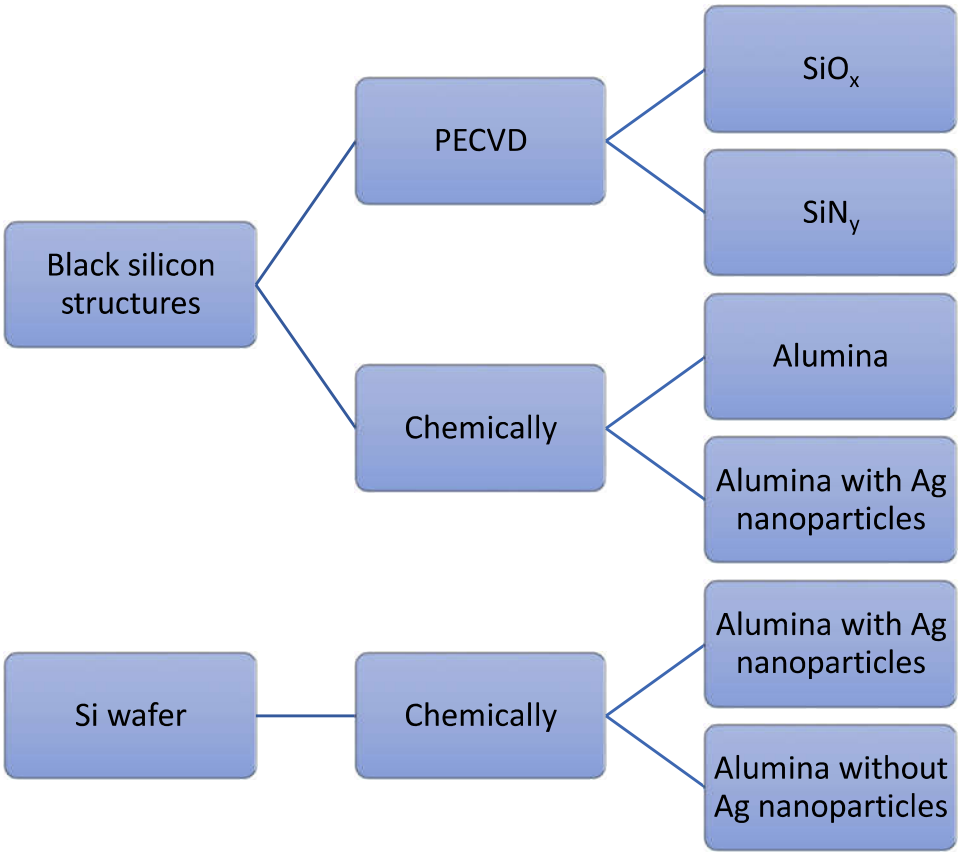

Figure 3.1. Shows the different tested production methods for passivating the black silicon structures.

All the samples were investigated structural, with SEM and/or S(T)EM, and optical, with spectrophotometer. The samples that were made without the black silicon structure, but with alumina passivation layer, were created for characterization of the plasmonic nanoparticles. Multilayers were not investigated in this thesis.

3.1 Producing the black silicon structure

All samples were based on 2" wafers that were polished on one side, had a thickness of 275 (+/- 25) µm and resistivity of 0.01-0.02Ω cm. The wafers were doped with boron (p-type) and had a (100) orientation[1].

[1] Wafers were purchased from «Silicon Materials"; http://si-mat.com/

All the samples were pre-cleaned to remove all the native oxides. The cleaning was done by immersion in HF solution of about pH=5 for 30 seconds. The HF solution contained 300ml deionized water and two drops of 0.85M HF. Then the samples were rinsed in isopropanol (IPA), rinsed in deionized water (DI water) and dried with N_2 gas.

Silver particles worked as catalysts for the chemical reaction. They were deposited on the wafers by immersing the samples in 5M HF and $AgNO_3$ (1:1) for 20 seconds. The wet chemical etching step was conducted in an ice bath, so the solution was approximately 7-8°C, for 20 min. Samples were immersed in a solution of 5M HF and 30% H_2O_2 (10:1). The hydroperoxide worked as an oxidizing agent for the process.

The silver particles were removed with a rinse in IPA, before being immersed in HNO_3 for 15 min and rinsed in DI water.

3.2 Deposition of passivation layer

One of the two passivation methods that was investigated was PECVD. The deposition rate with PECVD was varying for different layer thicknesses. Silicon oxide or silicon nitride were used in the PECVD method. The other method that was tested was chemical deposition of alumina. Some of the samples had silver nanoparticles within the alumina, for a plasmonic effect.

3.2.1 PECVD

PlasmalabSystem100, Oxford Instruments was used for the PECVD method. Different materials were tested; SiO_x and SiN_y with different parameters. The instrument was a direct PECVD, with a high frequency of 13.56MHz. Following values are given in *sccm* or standard cubic centimeter per minute (cm^3/min).

3.2.1.1 Silicon oxide

The amount of SiH_4 was decreased from the general recipe to decrease the deposition rate of the plasma. The system for the PECVD started with N_2 purge before the deposition of the passivation layer. The recipe for the deposition contained 2sccm SiH_4, 710sccm N_2O and 161.5sccm N_2. The temperature in the chamber was set to 300°C and the pressure 1000mTorr. The deposition time varied with 15, 30, 45 and 60 seconds, to get different thicknesses of the passivation layers. The recipe had a theoretical deposition rate of approximate 40nm/min. The chamber was purged three times with N_2, after deposition, to avoid contaminations before evacuating the chamber. Structural characterization of the surface was done before and after application of the passivation for comparison.

3.2.1.2 Silicon nitride

When depositing a passivation layer of silicon nitride, a mixture of 20sccm SiH_4, 20sccm NH_3 and 980sccm N_2 was used. The mixture, with a temperature set to 300°C and a pressure of 650mTorr, had a theoretical deposition rate of approximately 10nm/min. Four different deposition times were tested, 60, 120, 180 and 240 seconds, to achieve different thicknesses of the layers. This recipe had also one N_2 purge before and three after the deposition.

3.2.2 Alumina

The alumina solution (Al Sol) was created by dissolving aluminum nitrate ($Al(NO_3)_3$) in ethanol, with a Al:Ethanol(solvent) ratio of 1:20. An additive was used to create a stable solution and eliminate possible cracks in the films during the annealing process. Acetylacetone (AcAc) is a good additive with good chelating ability with aluminum. The AcAc was added to the solution and then stirred for approximately 18 hours, at room temperature. The ratio of AcAc and Al was 2:1. The solution was stable without any large physical changes, besides the sol getting a light orange, transparent color. The solution was stored in a fridge for several months, without any visible changes, during the project.

A sample was dip coated in the alumina solution and pulled out of the sol with a constant speed of 40mm/min. Then the sample was dried at RT before heat-treated at 110°C for 30 min, creating a dry gel film at the surface. Finishing off with an annealing for 3 hours at 600°C to form the alumina passivation layer. The sample were heated at a rate of 2.0°C/min and cooled with a cooling rate of 3.3°C/min. The annealing started and ended at 38°C. The annealing process is illustrated as an orange curve in Figure 3.2. A clean furnace, Super kanthal 3, was used for the annealing. All samples were covered with a lid, to prevent contamination during the annealing.

3.2.3 Deposition of Ag plasmon nanoparticles

Silver nitrate was dissolved in ethanol and heated to 40°C so that the silver nitrate was completely dissolved, before being mixed with the alumina solution. The solution of alumina with silver nanoparticles had a concentration of approximately 0.02M of silver. The sample preparation was done with the same procedure as for deposition of the chemical alumina passivation layer; dip coating with a speed of 40mm/min, dried at RT, dried for 30min at 110°C, however, the annealing was done at four different temperatures, see Figure 3.2. The annealing started and ended at 38°C. All the samples had a heating rate of 2.0°C/min, annealed for 3 hours and then cooled down with a rate of 3.3°C/min. The annealing temperatures that were tested was 450, 600, 750 and 900ºC.

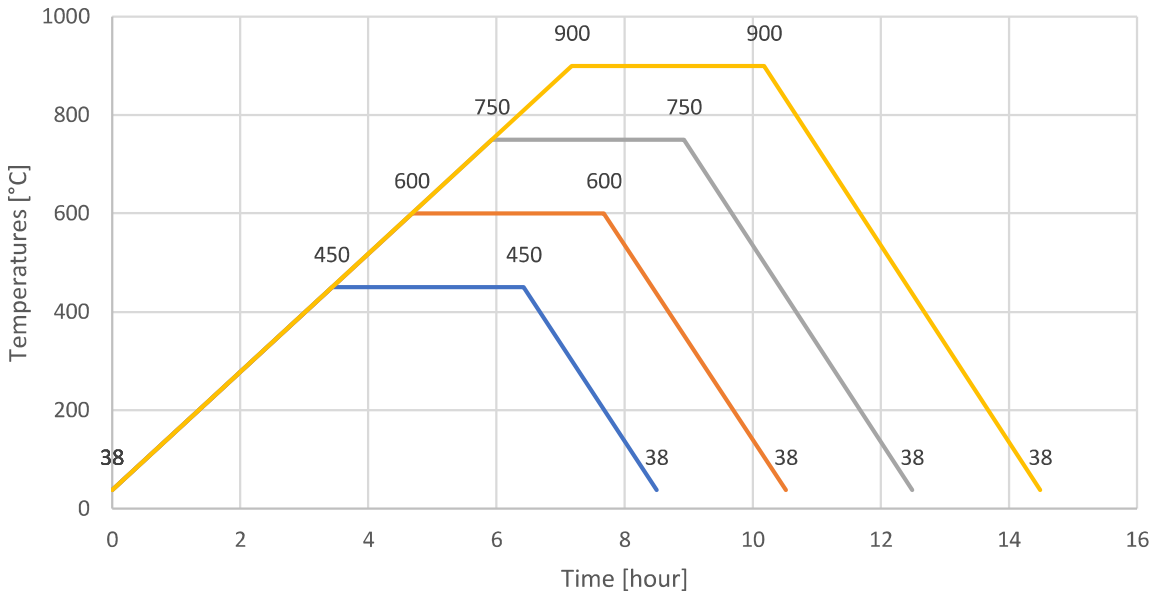

Figure 3.2. Illustration of the annealing of black silicon structure wafers that had been deposited with alumina and Ag nanoparticles. The samples were annealed with four different temperatures; 450, 600, 750 and 900°C, for 3 hours. Heated with a constant rate of 2°C/min and cooled down with 3.3°C/min.

Some extra samples were made for comparison, without black silicon structure. One sample with alumina passivation layer and silver nanoparticles. One sample with the alumina passivation layer, but without the silver nanoparticles. The purpose is to compare the different samples and hopefully see some effect from the silver nanoparticles. All these samples were created the same way with dip coating, heating and then annealing. An overview is illustrated in Figure 3.3.

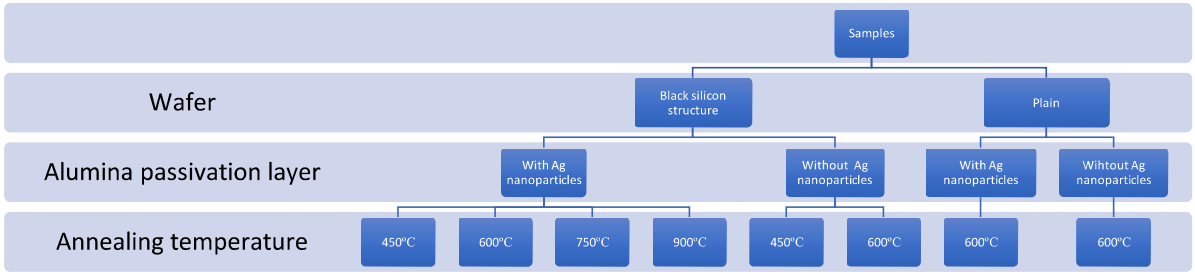

Figure 3.3. Overview of the samples with and without Ag nanoparticles in the alumina passivation layer, with different annealing temperatures. Two samples were created without the black silicon structure, marked as "plain".

3.3 Characterization

If the measured lifetime of the sample is low, it can be concluded that the recombination is high. The lifetime for all the samples was measured with µPCD. The different parameters were evaluated from the structural characterization, both surface and the cross-section. All

samples were measured regarding the optical and the structural properties. One of the samples with Ag nanoparticle was also investigated in transmission electron microscope (TEM). The structure was scratched of with a scalpel, creating a powder. The powder was investigated in S(T)EM and in TEM. The purpose was to determine an approximately mean size of the nanoparticles and their distribution. EDS was used both in the scanning electron microscope (SEM) and the TEM, as an attempt to determine the chemical elements in S(T)EM and to determine the properties of the silver nanoparticles in TEM.

3.3.1 µPCD and QSSPC

The lifetime of the samples was measured with a microwave photoconductivity decay (µPCD), Semilab WT-2000PVN. The instrument is used to measure the resistance as a function of time, therefore measuring the time dependent of the carrier concentration, indirectly measuring the lifetime. The reflection of microwaves is measured after the sample is illuminated with a short light pulse, which determines the minority carrier lifetime by the photoconductive decay. The light pulse generates excess carriers within the wafer, which increases the wafer conductance. The excess carrier will then recombine within the bulk and at both surfaces of the wafer and the conductance will decay to its initial value. An advantage with this method, is that it is not in contact with the samples. Equation 7 can be used for the measurements, where the lifetime is defined by dividing the excess minority carrier concentration on the recombination rate.

Some samples were also measured with a quasi-steady state photoconductance (QSSPC), BCT-300 from Sinton Consulting, inc. These measurements were done with regards to the electron-hole-pair (EHP) steady-state generation-recombination balance, which means a nonequilibrium condition, all processes are constant and balanced by opposing processes[24].

Both methods measure the lifetime of the wafer and can therefore give an indication on the recombination losses for the sample. Low recombination will give a longer lifetime. Since there is some restriction regarding the sample size for QSSPC measurements, was only some of the sample measured with this method.

3.3.2 SEM, S(T)EM and TEM

Two different scanning electron microscopes(SEM) were used. The nanostructure was characterized with secondary electron detection in FESEM, Zeiss Ultra, 55 Limited Edition and/or Hitachi S-5500 S(T)EM. The SEM was mainly used for the surface characterization and S(T)EM was used for the cross-section and for characterization of the silver plasmonic nanoparticles. Low accelerating voltage, 10-15kV, was chosen, because of the short

nanostructure on the surface. The surface was inspected for visible impurities or defects, before taking the images. All the surface images had the same magnification, for easy comparison; 1, 3, 5, 10, 20 and 35k.

The cross-section characterization was done with Hitachi S-550 S(T)EM. The samples were broken with a diamond scriber, before looking at the cross-section of the nanostructure. Since all the wafers are of monocrystalline silicon, with the specific orientation of (100), all the samples should have clean breaks. The samples with the black silicon structure contradict this statement. Some samples were hard to break and there was rarely a clean break. This can make it difficult to achieve an accurate conclusion, since the structure might be destroyed in the preparation process for the cross-section images. All the samples were placed in a homemade holder and glued with carbon glue. Since these sample holders were homemade, the quality of the measurements might be incongruent. An approximate thickness of the passivation layer and nanostructure was measured. Figure 3.4 illustrates an example of some of these measurements for one of the samples.

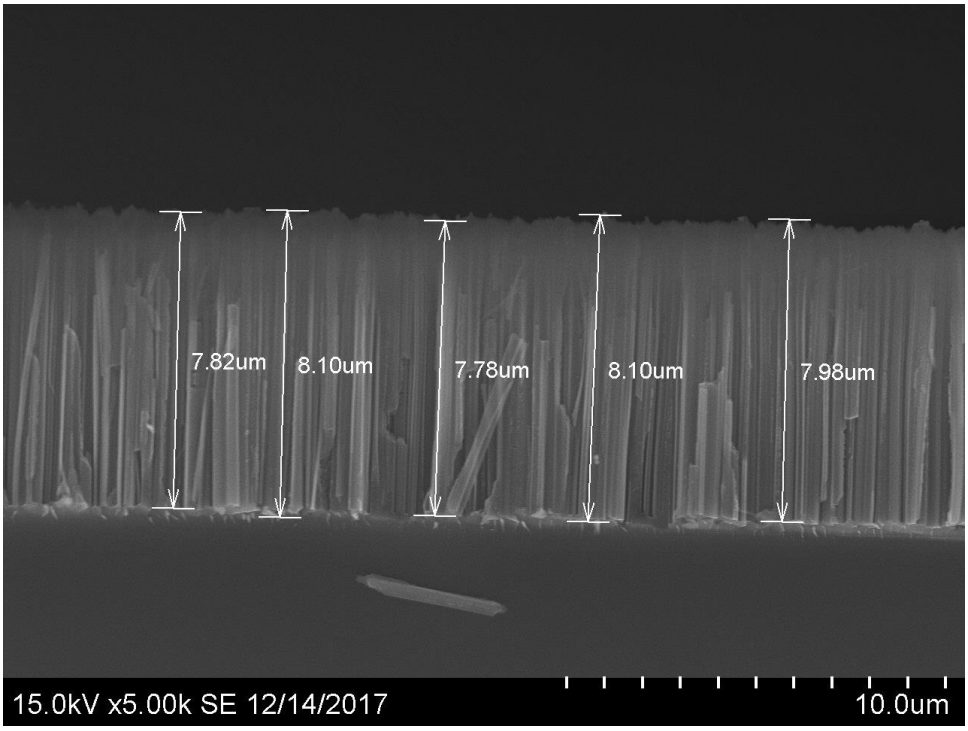

Figure 3.4. Example of measurement done of the thickness of the nanostructure. These measurements were done to calculate an approximate average thickness. The average thickness was then plotted with standard deviation.

The measurements were done from the top of the nanostructure to the start of the substrate. Several measurements were done for each sample to calculate an average thickness. The nanostructure was measured from the top of the nanostructure to the beginning of the

substrate. The calculations were plotted with a standard deviation. The measurement tool was a built-in function in the program that was used for the S(T)EM.

S(T)EM was not sufficient for determining the characteristics of the Ag plasmon nanoparticles. Therefore, the samples with deposited silver nanoparticles were also investigated in a Transition Electron Microscopy (TEM). The nanostructure, with alumina and Ag nanoparticles, was scratched of and studied as a powder. The "powder" was placed in a holey cobber grid with carbon film, by scratching the structure on a tissue, soaking it in ethanol and then put the grid on top so it could "soak" up the nanostructure. The sample were then investigated in Jeol JEM-2100 electron microscope, with accelerating voltage of 200 kV.

The silver particle content was measured with EDS in the TEM and compared with areas without any visible silver nanoparticle. EDS measurements were also taken over different "nanostructure-bundles". The purpose was to see if there were a clear difference between the outer layer and the core of the structure and determine the difference between the alumina passivation layer and the silicon core. The filament for the TEM that was used, was LaB6-filament.

Energy-dispersive x-ray spectroscopy (EDS/EDX) was used to investigate the passivation layer and silver nanoparticles at the surface. EDS gives an element mapping of the surface. Measurements was done in S(T)EM, of some of the surfaces and the cross-section, and in TEM. Some values for different elements, that give distinct peaks in EDS, are listed in Table 1[2].

Table 1. Peak values for relevant chemical elements, for EDS measurements

Chemical Element	**Si**	**Al**	**O**	**N**	**C**	**Cu**	**Ag**
K_α [keV]	1.74	1.49	0.53	0.39	0.28	8.04	
L_α [keV]						0.93	2.98

These values will help characterizing the different peaks in the spectrum and evaluate possible chemical elements. It is a list of all the elements that are being used in the samples or for preparation for the characterization. Carbon, C, i.e., is listed because of the carbon glue that is being used. It might give some disturbance for the measurements. The same is for Al, since the sample holder is made of aluminum. Some spectrums were compared to determine if the

[2] These values are from the energy table from the webpage belonging to jeol; https://www.unamur.be/services/microscopie/sme-documents/Energy-20table-20for-20EDS-20analysis-1.pdf (18.01.18)

passivation layer had been successfully applied. All EDS measurements had a disturbance/noise peak around 0eV energy, at the x-axis.

3.3.3 Spectrophotometer

The reflection of each sample was measured with a spectrophotometer. The instrument "shot" light with different wavelengths on the sample and then measured the percentage of reflected light. The result is a function of reflection regarding different wavelengths. The instrument was a Perkin Elmer 1050 with a 150-integrated sphere that detects the reflected light in all directions or the total reflection. All the optical graphs will have a disturbance around 850nm. This is due to a change in detections in the spectrophotometer and is causing some disturbance in the data around this point. The machine detects wavelengths from 280 to 2500nm, with a 5nm step length. Light with energy much larger than the bandgap will start to transmit through the sample, giving misleading results. The results that are being included and evaluated is therefore only up to 1200nm.

4 Results and discussion

Black silicon structure was successfully produced with metal-assisted wet chemical etching. All the samples appeared black after the final cleaning. Structure and optical characterization helped determining the different effects of the varying parameters for the different deposition methods. Spectrophotometer was used for measuring the reflection, which should be kept below 1% after deposition of the passivation layer. Results from the lifetime can give an indication of whether the passivation layer have any effect as short lifetime indicates high recombination. The lifetime was measured with µPCD and some samples used QSSPC, additionally. There were only created one sample with each parameter, because of time and material restriction. Several samples should have been created for each parameter, characterized and then compared, for a more accurate conclusion.

The structures were characterized with surface and cross-section images. All the cross-sections were measured, for an approximately thickness of the nanostructure with and without the passivation layer. The measurements are just rough estimates. The thickness would be measured in micrometers and deposition can happen in nanometers. There might be no substantial structural difference, even though the passivation layer has been applied successfully. There is a large margin of error since all samples was placed in homemade sample-holders. When observed at in the microscope, the cross-section samples were tilted, for a close to right-angled view of the cross-section. During preparation of the samples there were rarely a clean break for the samples with black silicon structure. This results in an uneven cross-section surface and gave deviations when calculating the thickness. There is a challenge to get an accurate interpretation of the cross-section, since there are several difficult steps of preparation that can end with misleading results. The measurements are just an indication if there has been a difference in the nanostructure after the passivation layer.

The black silicon structure was characterized before depositing passivation layers and plasmon nanoparticles. The structure and reflection data were used as a reference for the experimental work and as comparison for all the other samples. Figure 4.1 shows the cross-section (a) and surface (b) images of the black silicon structure, both with 5k magnification.

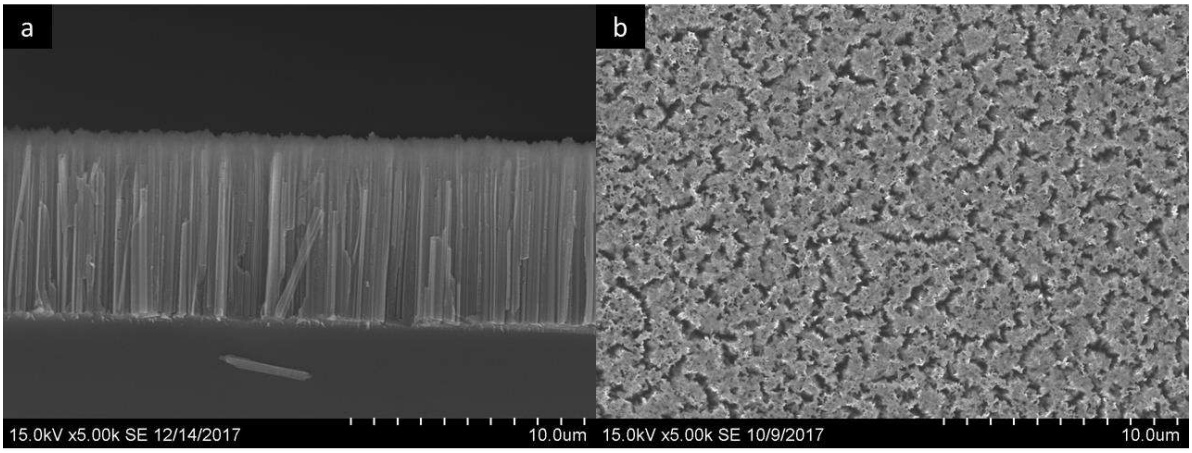

Figure 4.1. Cross-section (a) and surface (b) images of the black silicon structure that have been used as basis. Both images have a 5k magnification. Image (a) of the cross-section have the substrate located at the bottom, under the nanostructure.

The samples were successfully reproduced, with the same recipe used in the specialization project. The cross-section image shows a needle-like nanostructure that is approximately 8µm thick. Image 4.1*b* indicate a good and uniform distribution of the nanostructure. It appears that the nanostructure has smaller "holes" within the structure and larger channels in the nanostructure. In the cross-section image, Figure 4.1*a*, it looks as if the nanowires gather at the top of the nanostructure corresponding to the surface image, 4.1*b*. A successful passivation layer should be deposited homogenous over the whole nanostructure, within the needle-like nanostructure.

4.1 PECVD

Both silicon oxide and silicon nitride passivation layers appeared to have been deposited successfully with PECVD. Most of the samples appeared, visually, to have kept the same nanostructure after passivation. The measurements done with the spectrophotometer, showed that the optical properties of the samples with SiN_y, varied with the thickness of the deposition time. This appears to almost be the case for the SiO_x as well. Surface and cross-sections images have been considered for the structural characterization. An approximate thickness of the nanostructure with passivation layer have been measured from the cross-section images.

4.1.1 Silicon oxide

A passivation layer of silicon oxide was deposited on four different samples with PECVD, with four different deposition times: 15, 30, 45 and 60 seconds. The amount of SiH_4 was low, to decrease the deposition rate. A short deposition time was chosen so that the passivation layer should, theoretically, have a thickness of approximately 10-50nm. The intention was to prevent the pits from closing.

The surface of the samples was characterized with SEM images before and after deposition of the passivation layer. The SEM images showed that the passivation layer was uniformly distributed over the surface, within the nanostructure. Figure 4.2 shows the surfaces of all the four different samples with two different magnifications. The surface looks similar, when compared with image 4.1*b*.

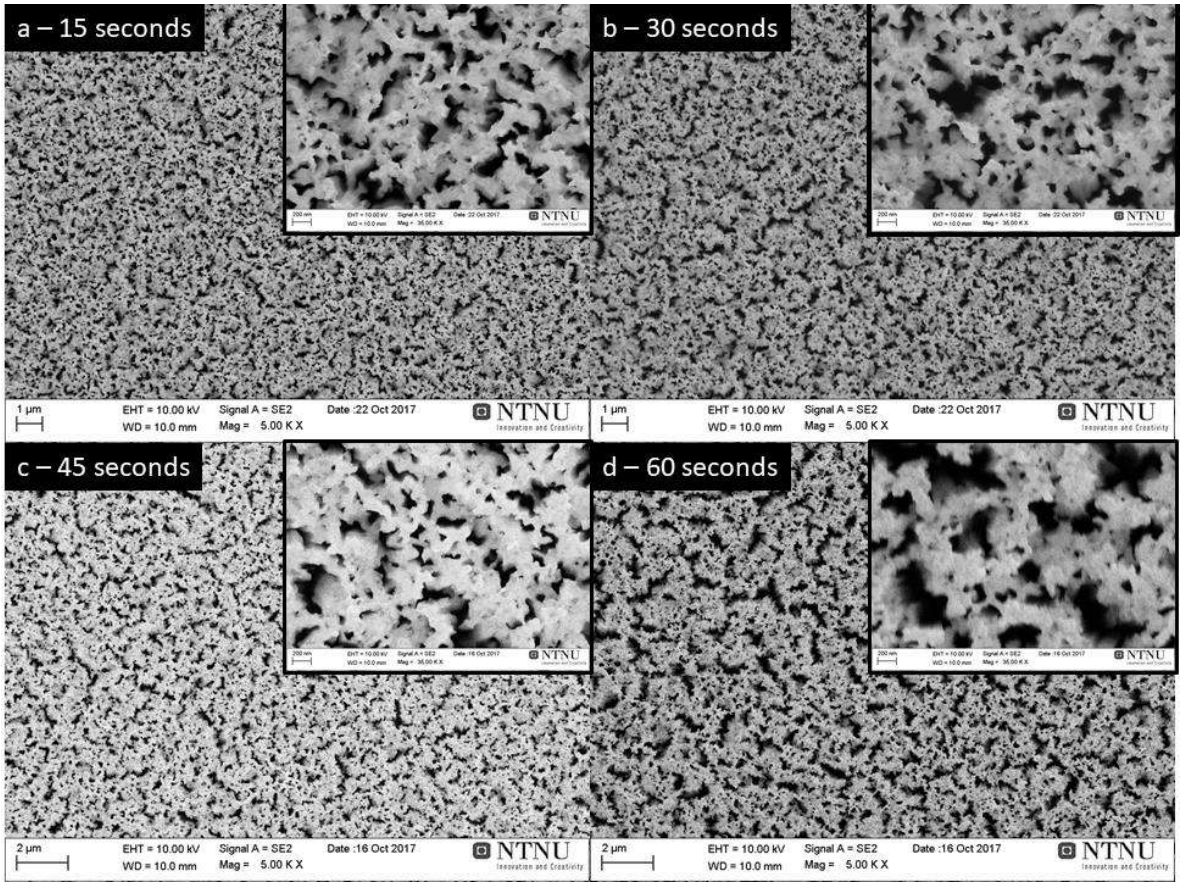

Figure 4.2. Surface images with different deposition times, marked in each corresponding upper-left corner. The magnification was 5k and 35k for the small images in the upper-right corner.

All the large images have a magnification of 5k and have a smaller image, in each corresponding upper-right corner, with magnification of 35k. The structure looks similar for all the samples, with both the channels and the small "holes" within the nanostructure. These images show a successful deposition of the passivation layers. A change is observed in the coarseness of the structure, when comparing the different surface images to each other, in Figure 4.2. The shortest deposition time (15s), Figure 4.2*a*, has the finest structure and then it becomes coarser with longer deposition time. The difference in coarseness for the nanostructure appear the best when comparing 4.2*a* and 4.2*d* (15 and 60 seconds). This makes sense, since the passivation layer should become thicker with longer deposition time and therefore "thicken" the nanostructure. It appears to be a refining of the structure, when

passivating with silicon oxide, and then the passivation gets thicker with longer deposition time. It is not possible to determine if this refining, most likely a chemical reaction, happens in the PECVD chamber, before deposition of the plasma or after. The nanostructure should not react with the N_2 gas that is being used for the purge. The most promising conclusion is that by passivating the silicon oxide, there are a chemical reaction occurring at the surface.

Figure 4.3 shows the surface structure before (4.3*a*) and after (4.3*b*) deposition of silicon oxide with PECVD for the sample that had a deposition time of 60 seconds. Besides the degree of fineness of the structure, there are no visual difference between the samples before and after deposition of the passivation layer.

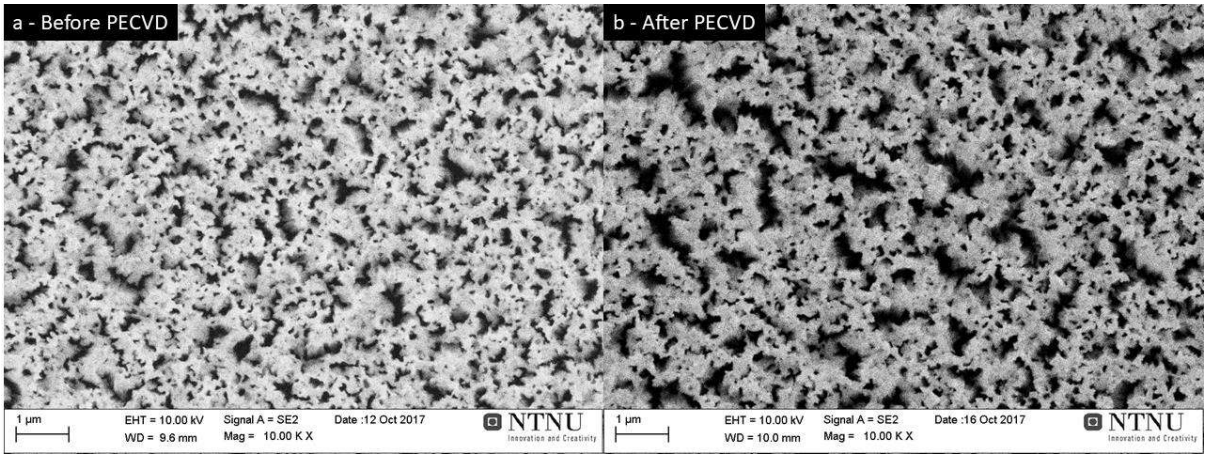

Figure 4.3. The surface before (a) and after (b) deposition of silicon oxide with PECVD. Both images are taken with 10K magnification in FESEM Zeiss Ultra 55. The image(b) are of the surface for the samples that had a 60 second deposition time, which was the longest deposition time for the silicon oxide samples.

The sample that was deposited with deposition time of 60 seconds is used as an example for all the other three samples with shorter deposition time. The surface structure is very similar after deposition (4.3*b*), when compared to the sample before deposition (4.3*a*). The coarseness is almost the same in these images. It can be assumed that the sample with the shortest deposition time (15s) have a much finer nanostructure than before the deposition of the passivation layer.

The cross-section images, Figure 4.4, shows more varying structures between the different deposition times.

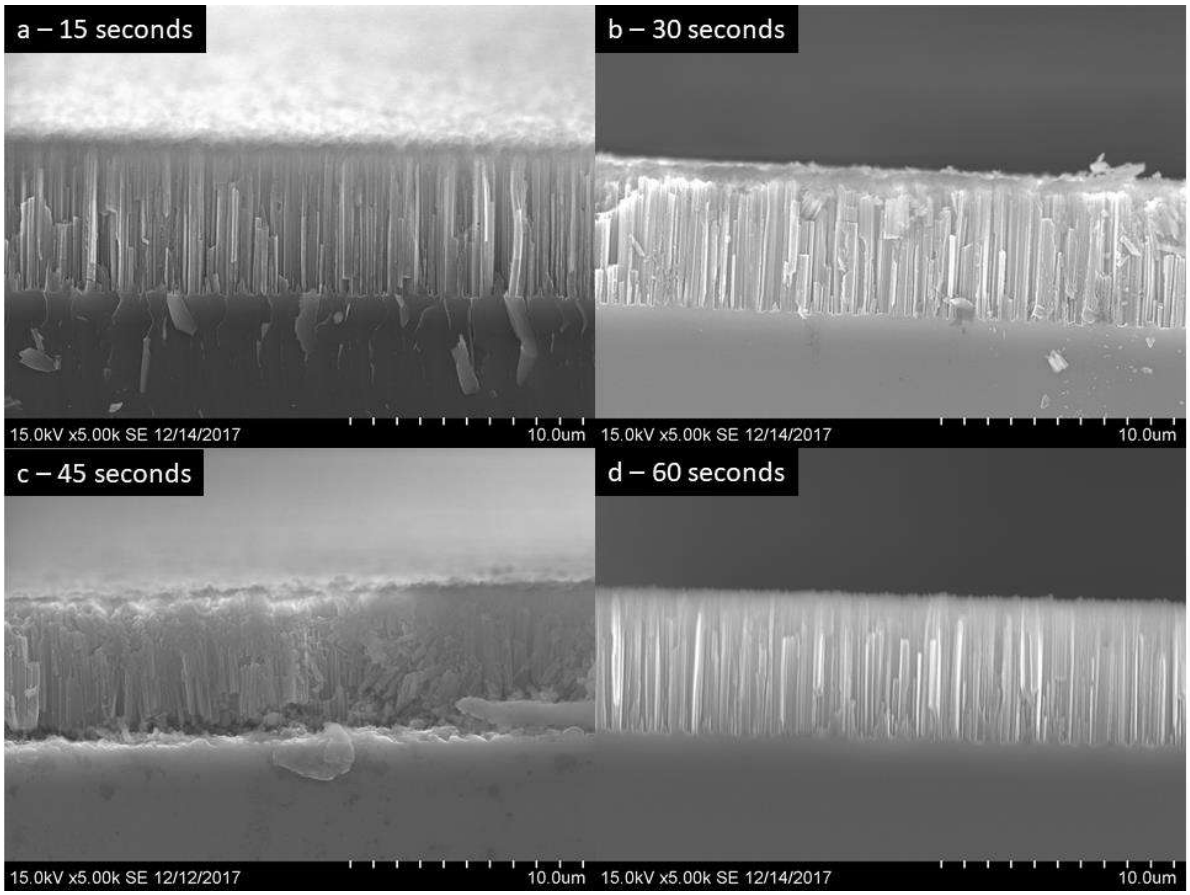

Figure 4.4. Cross-section images of the nanostructure after deposition of SiO with PECVD. The different deposition times is indicated in each accompanying upper-left corner. The images have a 5k magnification. The substrate is located at the bottom, under the nanowires in all the images.

The shortest and longest deposition times have the straightest and most visually promising cross-section structures. The samples with deposition times of 30 and 45 seconds are broken to different extents. It can be assumed that the illustrated structures show misleading results, since samples with shorter and longer (15 and 60s) deposition times than these two (30 and 45s) have a complete cross-section structure. The broken structure can have been caused by poor preparation of the samples. The carbon glue can have been spilled on the cross-section, because of difficult preparation, and therefore giving misleading results. The nanostructure can have been damaged when the wafers were broken during preparation. If these cross-section of 4.4*b* and 4.4*c* were accurate representation of the nanostructure, that should have been detected in the surface images, 4.2*b* and 4.2*c*.

Figure 4.5 illustrates the different measured thicknesses of the nanostructure with passivation layer. The measurements are plotted with average thickness as a point with standard deviation. All the measurements that is done are rough estimates of one sample, at two different random spots.

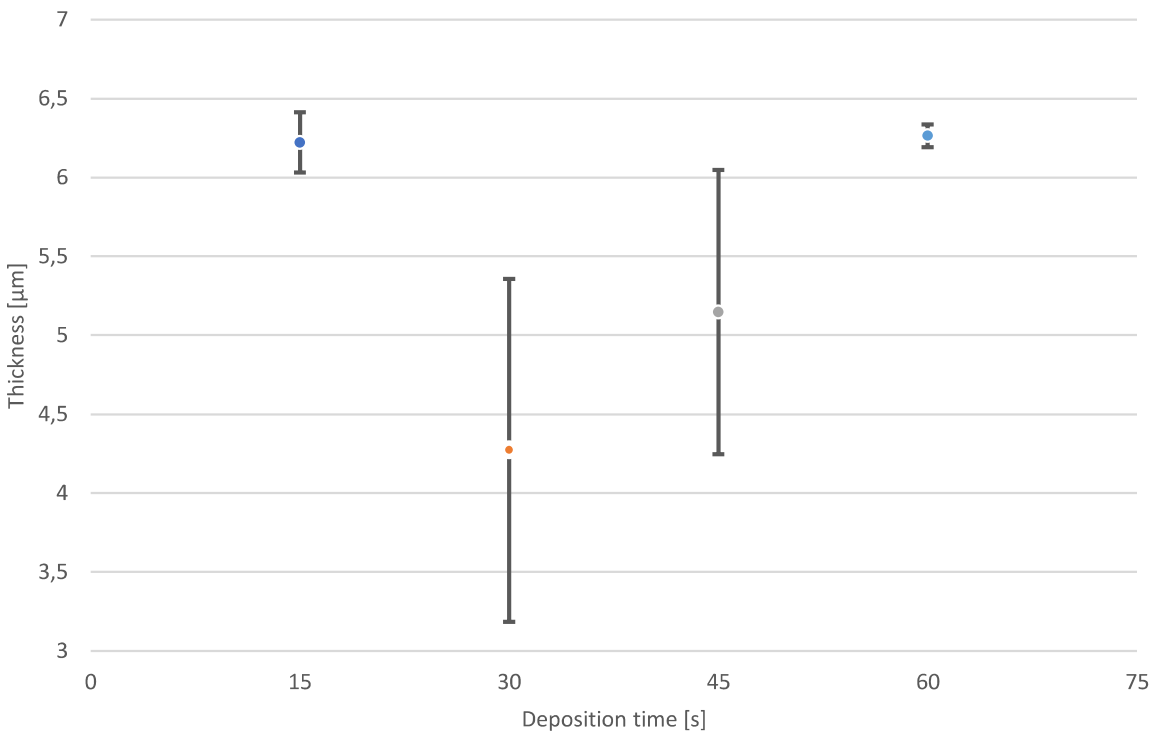

Figure 4.5. Measured thickness for the nanostructure with SiO_x passivation layer is marked as points with corresponding standard deviations.

The thickness of the nanostructure with passivation layer have been significantly reduced, from the original thickness of approximately 8µm. All samples with silicon oxide passivation layer on the nanostructure have an average below 6.5µm. Between the samples there are no clear pattern regarding the thickness. For the samples with deposition time of 30 and 45 seconds, there are a great deviation between the measured thicknesses. There is a noticeable similar thickness for the longest and shortest deposition time. If there was a difference regarding a coherence with increasing deposition time, it should be noticed between these. Even though there is a small difference between the 15 and 60 seconds deposition times samples, regarding the thickness, the passivation layer can have different thickness at the nanoscale. The thickness may have been so short that it was not detected for these samples. The thickness for deposition times of 30 and 45 seconds are affected by the possible poor preparation. Since the shortest and longest deposition times have approximately the same average thickness, it could be assumed that there should be a coherency with the intermediate deposition times.

The significant change in thickness can be caused by either mechanical or chemical events. There were no visible residue or traces on the surface or in the chamber after deposition, so a mechanical accident can most likely be ruled out. A chemical reaction can have happened

within the nanostructure, causing the reduction in thickness. The surface structure also showed a finer structure for the shortest deposition time, which also can be caused by a chemical reaction. The chemical reaction refined the structure for the shortest deposition time and then the passivation gets thicker for longer deposition time, resulting in a coarse surface structure and a thicker nanostructure. Both the surface and the optical characterization shows promising results for the silicon oxide passivation layer. A conclusion will therefore be based on the cross-section images. For a more complete conclusion recombination should be taken into consideration.

The optical characterization of the samples with a silicon oxide passivation layer, showed overall good results. The measurements were done with spectrophotometer, which measures the percentage of reflection for different wavelengths. Figure 4.6 illustrates the reflection, which was not significantly higher for any of the samples.

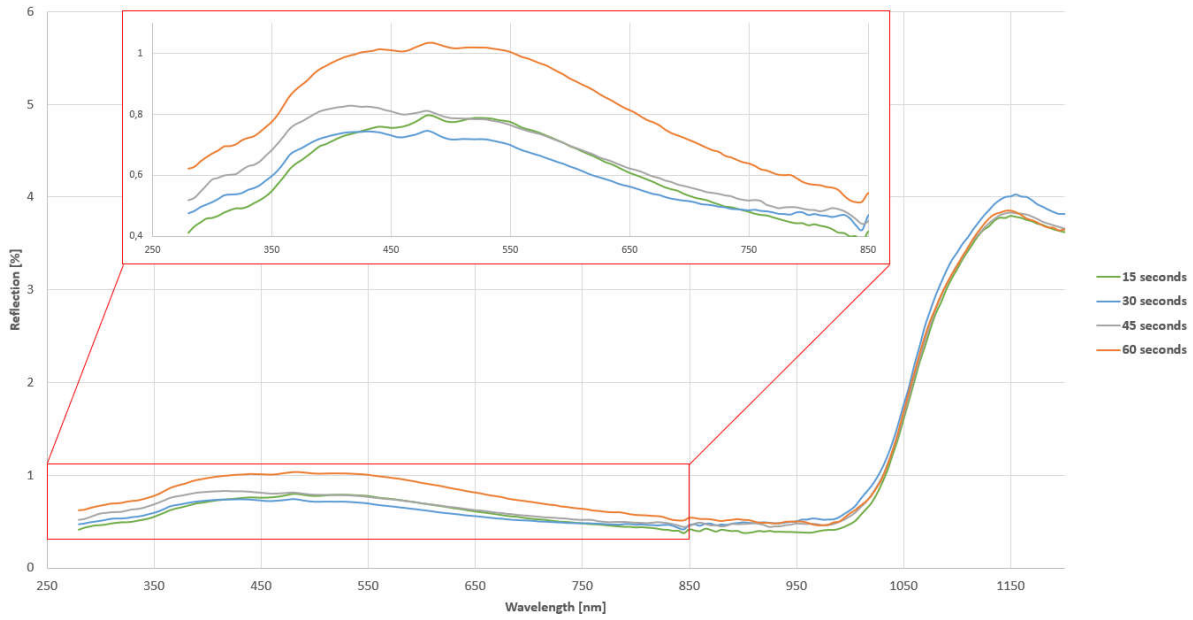

Figure 4.6. Percentage of reflection for different wavelengths for the four samples that were passivated with silicon oxide, with PECVD. The different deposition times should have created different thickness of the passivation layer.

All the samples had a reflection ≤ 1%. The sample with the longest deposition time (60s) had the highest reflection, around 1%, which is slightly higher than the other samples. It appears to be a coherence between thickness and reflection, besides the 15 seconds sample. The reflection increases slightly for increasing deposition time. The exception is the sample with deposition time of 15 seconds, that start as the lowest reflection, but increases more than the 30 seconds sample. The optical measurements show that the promising optical properties have been kept after deposition of a silicon oxide passivation layer.

4.1.2 Silicon nitride

Silicon nitride was passivated with PECVD on samples with black silicon structure. The surface images were taken with SEM. It showed that three of the structures were visually similar before and after the deposition. The sample with the longest deposition time got a grey-blue color on the surface. The three samples with the shortest deposition time, 60, 120 and 180 seconds, have kept the same structure after deposition of the silicon nitride passivation layer. The surface of the three samples is showed in Figure 4.7, with a 5k magnification. The deposition time is marked in the upper-left corner for each corresponding image. The sample that is marked with 0 seconds, is the black silicon structure on the surface prior to deposition, for comparison. Figure 4.7 shows that the structure has kept the nanostructure caves, with the small holes within the structure after passivation.

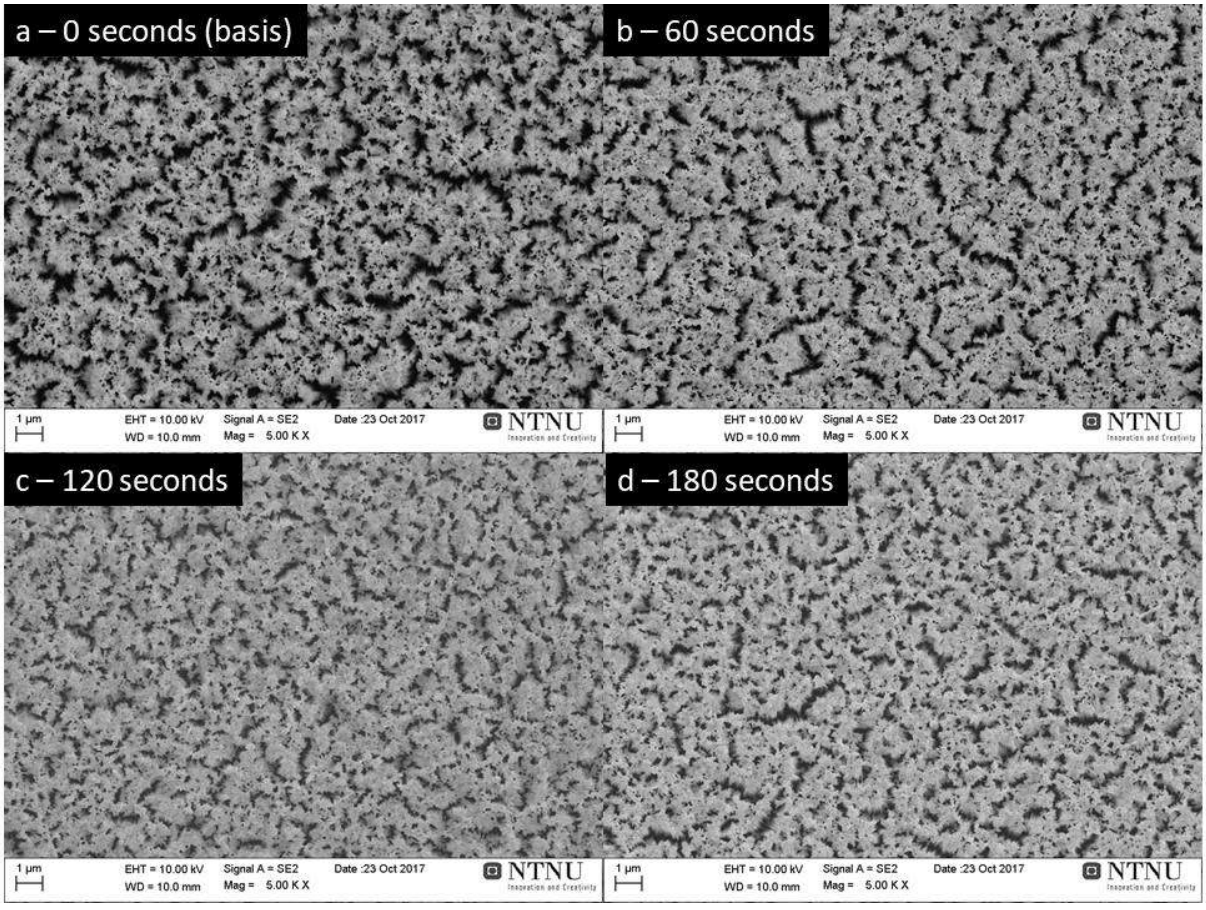

Figure 4.7. The surface of samples with different deposition times, all with 5k magnification. The deposition time is marked in the correspond image in the upper-left corner. The image with 0 seconds is the referance black silicon structure before deposition, for comparison.

It appears to be no visual variation for the surface images in Figure 4.7, regarding the deposition time. The nanostructure seems to have become slightly finer after deposition of the passivation layer, by comparing image 4.7*a* with 4.7*b-d.*

The sample with the longest deposition time (240 seconds) had a deviating structure. Figure 4.8 shows the surface with 1k(4.8*a*) and 5k(4.8*b*) magnification of the sample and the cross-section (4.8*c*). Cavities of varying sizes were discovered on the surface. Similar areas of these cavities were found for the cross-section image, Figure 4.9*c*. The cross-section of the sample showed both straight needle-like nanostructures and areas with these “holes” within the structure.

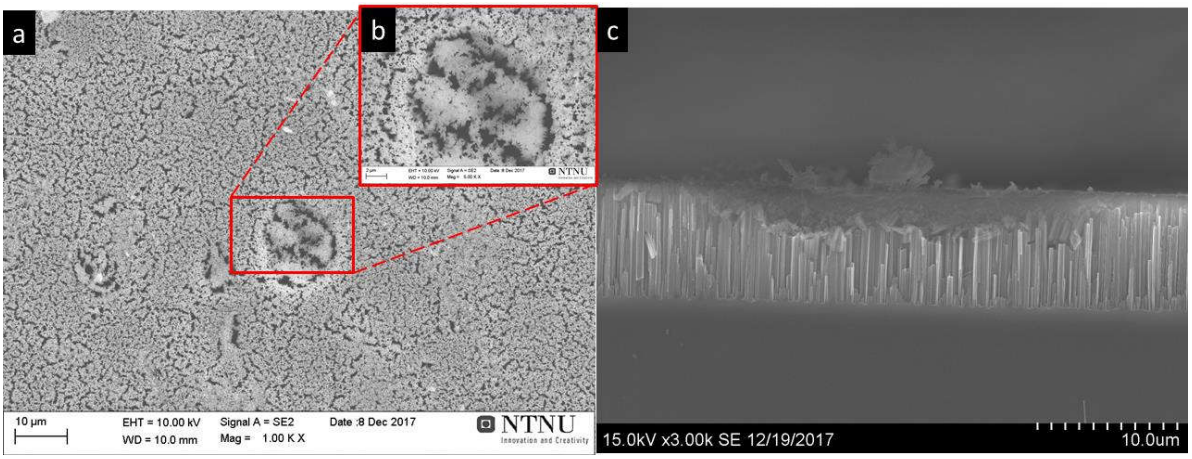

Figure 4.8. The surface, with 1k(a) and 5k(b) magnifications, for the sample with 240 seconds deposition time. The cross-section(c) shows a "hole" in the structure from the side. The substrate is located at the bottom, under the nanostructure, in the cross-section image(c).

These areas can be caused by contamination prior to deposition or a chemical reaction during storage of the samples. It has most likely been caused during or after deposition, since these areas was not found on the black silicon samples before deposition of the passivation layer. Both the surface and cross-section image of the sample, Figure 4.8, indicate that there must be a shorter than 240 seconds deposition time. Too long deposition time with silicon nitride with PECVD appears to destroy the nanostructure.

The cross-section images, Figure 4.9, of the sample with 60(4.9*a*) and 120(4.9*b*) seconds deposition time, have a straight, and overall promising, nanostructure. It appears to have kept the same features as before deposition of the passivation layer.

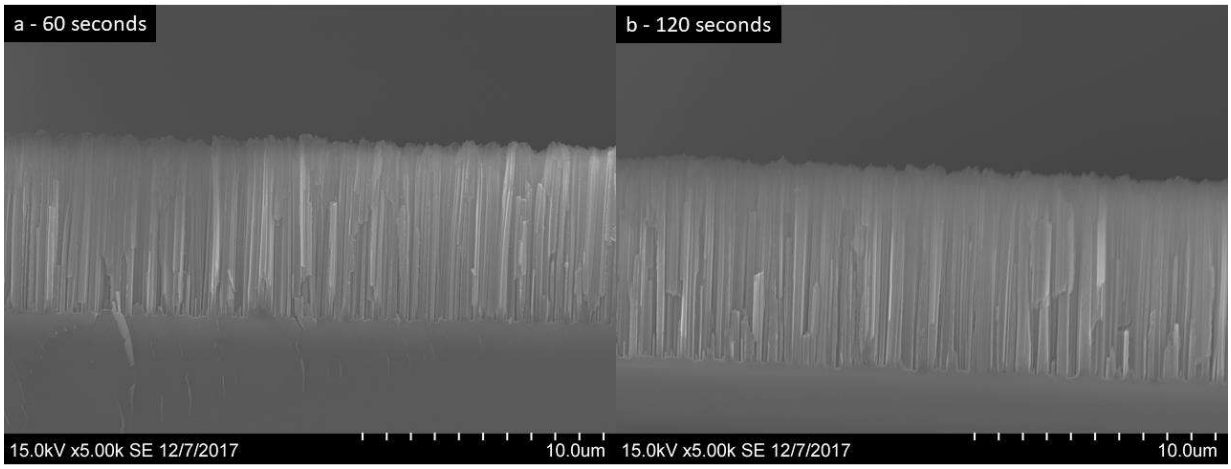

Figure 4.9. Cross-section image of the two samples with deposition time of 60 seconds(a) and 120 seconds(b). Both images have a 5k magnification and were taken with S(T)EM. The substrate is located at the bottom, under the nanostructure in both images.

The sample with 180 seconds as the deposition time has a different cross-section structure, showed in Figure 4.10. It looks as if the nanostructure has a "overhanging" of the structure. The needle-like nanostructure is sticking out, above the substrate. The red area of the structure in image 4.10*a* is enhanced with 25k magnification in image 4.10*b*. The fracture surface, in Figure 4.10*b*, looks brittle and as if the core of the structure contains a porous structure.

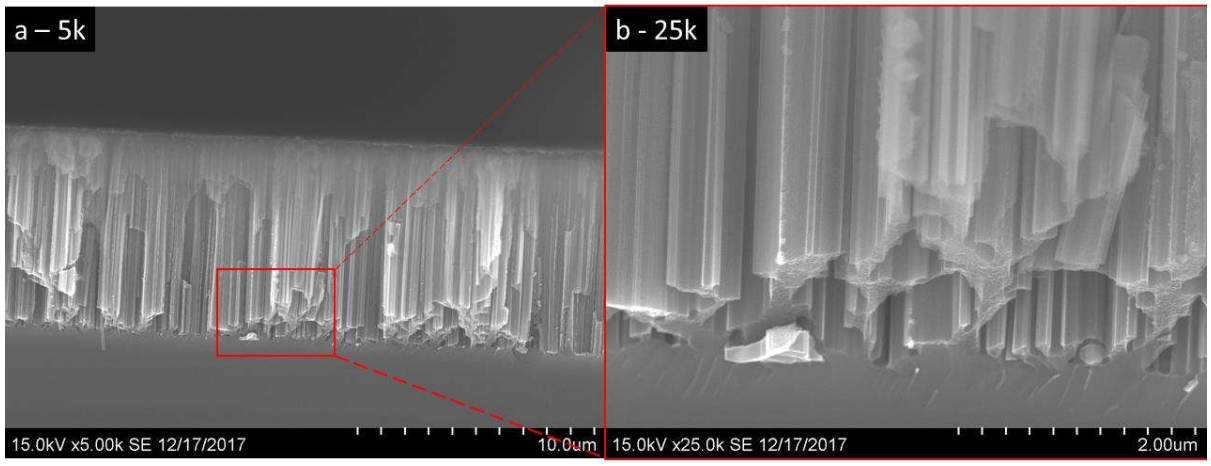

Figure 4.10. The cross-section image of the sample with deposition time of 180 seconds. 4.10a is with the 5k magnification and 4.10b is the red area enhanced with 25k magnification. The substrate is located at the bottom, under the nanostructure in both images.

The thickness of the nanostructure after deposition of a passivation layer was measured when taking the cross-section images. The measurements were done from the top of the nanostructure to the start of the substrate. This is approximate measurements but can give an indication on the thickness of the passivation layer, when comparing to the black silicon nanostructure. The average thickness is plotted with standard deviation in Figure 4.11.

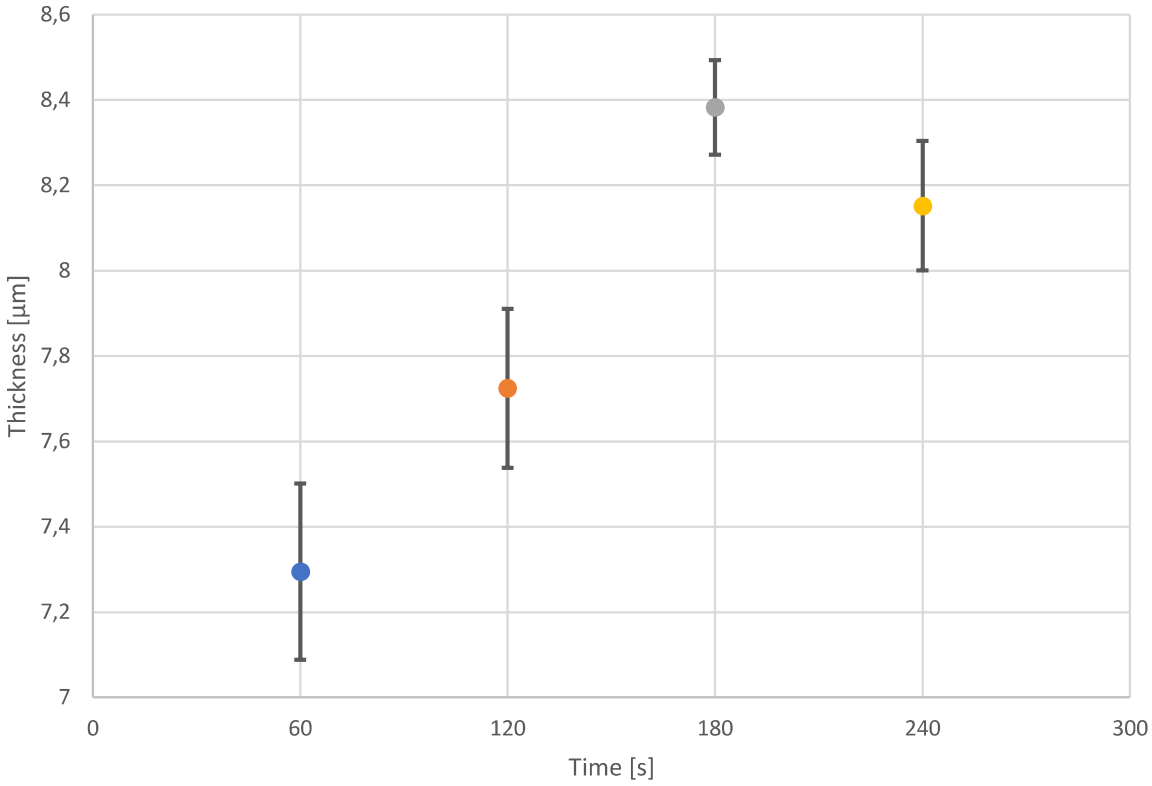

Figure 4.11. Average thickness with standard deviation for the four different samples. The average thickness of the nanostructure is marked as the point, for the different deposition time for samples with the SiN_x passivation layer.

The graph in Figure 4.11, shows that the thickness is varying with approximately two hundred nanometers. Overall, the thickness increases with an increased deposition time. The thickness is varying between 7 and 8.5 micrometers. The surface nanostructure was partly destroyed for the longest deposition time (240s), so here are the measurements done where the cross-section appeared to be a complete nanostructure, not including the holes. This might result in some deviations from the actual length. The thickness of the black silicon structure without any passivation layer was around 8µm. Figure 4.11 illustrates that the nanostructure of the samples with the shortest deposition times have in some way shrunk, compared with the black silicon structure. Same remarks can be done here as for the silicon oxide passivation layer. Since there were no residue after deposition or with the preparation, it can be assumed that there is a chemical reaction that have caused this change in thickness. Since this statement is valid for both PECVD methods, it should be investigated if the shrinking arises from the deposition method or passivation material. The nanostructure seems to shrink by using this method, with this material, and then thickens with longer deposition time.

The optical properties of the samples showed an increasing reflection with increasing thickness of the layer. Figure 4.12 shows that there is a coherency in the deposition time and the reflection.

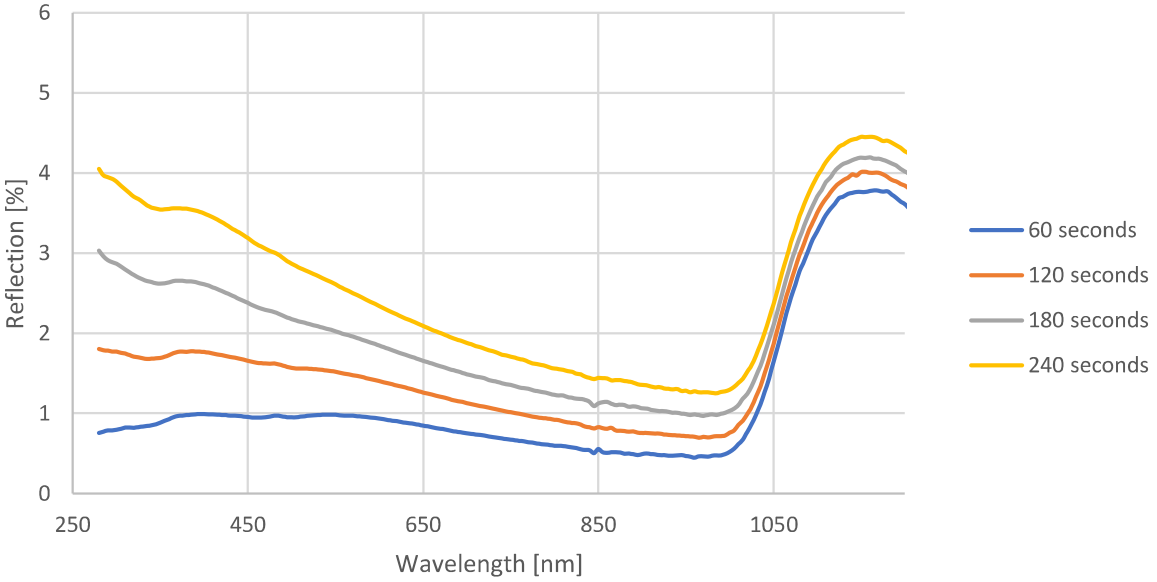

Figure 4.12. Samples passivated with SiN_y with different deposition times. The reflection is increasing with increasing deposition time or thickness.

An increasing deposition time increased the reflection of the samples. The sample that had a deposition time of 240 seconds reached almost 4% reflection. The sample that only had a deposition time of 60 seconds have kept a low reflection around 1%. From Figure 4.12 it can be determined that from these results, the shortest deposition time (60 seconds) is the most favorable. Before reaching a conclusion, the recombination should be taken into consideration. The sample that had a deposition time of 120 seconds have a reflection below 2% within visible light. This sample also had a visually promising structure, in both the surface and the cross-section. If the sample have a remarkable reduced recombination loss, compared to the 60 seconds sample, this sample could have an overall higher efficiency.

4.2 Chemical alumina passivation layer

The passivation layer of alumina was constructed successfully with chemical deposition, by dip coating the black silicon structure. This sample was created without the silver nanoparticles and annealed at 600°C for 3 hours. The surface (4.13*a*) and cross-section (4.13*b*) image is illustrated in Figure 4.13.

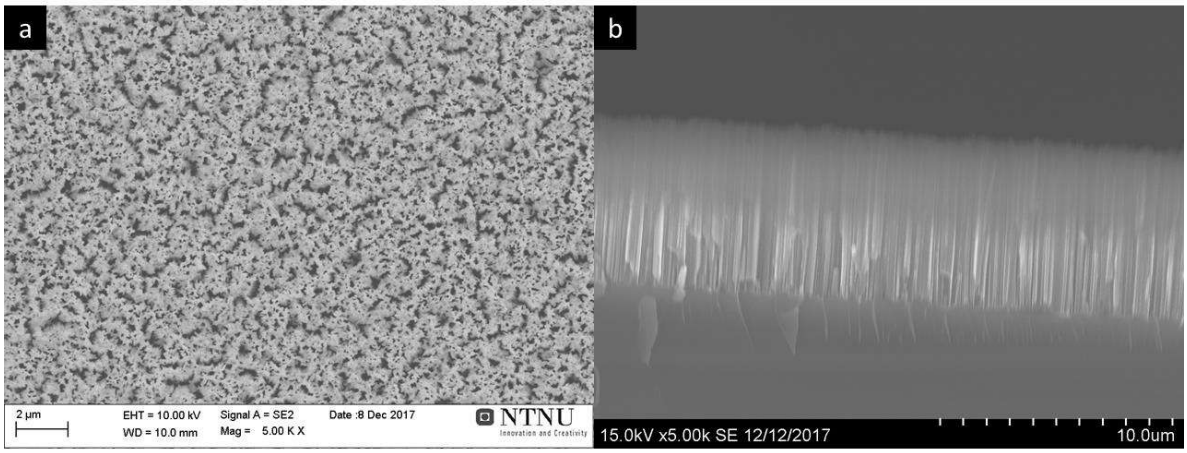

Figure 4.13. SEM images of the surface(a) and the cross-section(b) of the sample that was passivated with alumina and annealed at 600°C for 3hours. In the cross-section image(b) is the substrate located at the bottom, under the nanostructure.

Both images were taken with 5k magnification. The surface image 4.13*a* shows that the black silicon structure has been kept intact after the chemical passivation. There are the same caves and small holes within the nanostructure. The cross-section image, 4.13*b*, shows that the nanostructure has a straight needle-like structure. The average thickness of the nanostructure with the passivation layer was measured to be approximately 7.5µm (±0.073). This is also shorter than the original black silicon structure. Both mechanical and chemical explanations can be used analyzing these results. There might have been some mechanical residue left in the alumina solution after dipping the wafer, even though nothing was observed. A possible chemical reaction can also have occurred on the surface, resulting in a shorter nanostructure.

Figure 4.14 illustrates the reflection of the sample with alumina passivation layer, compared with the samples that had a 60 seconds deposition time with passivation layer SiO_x and SiN_y

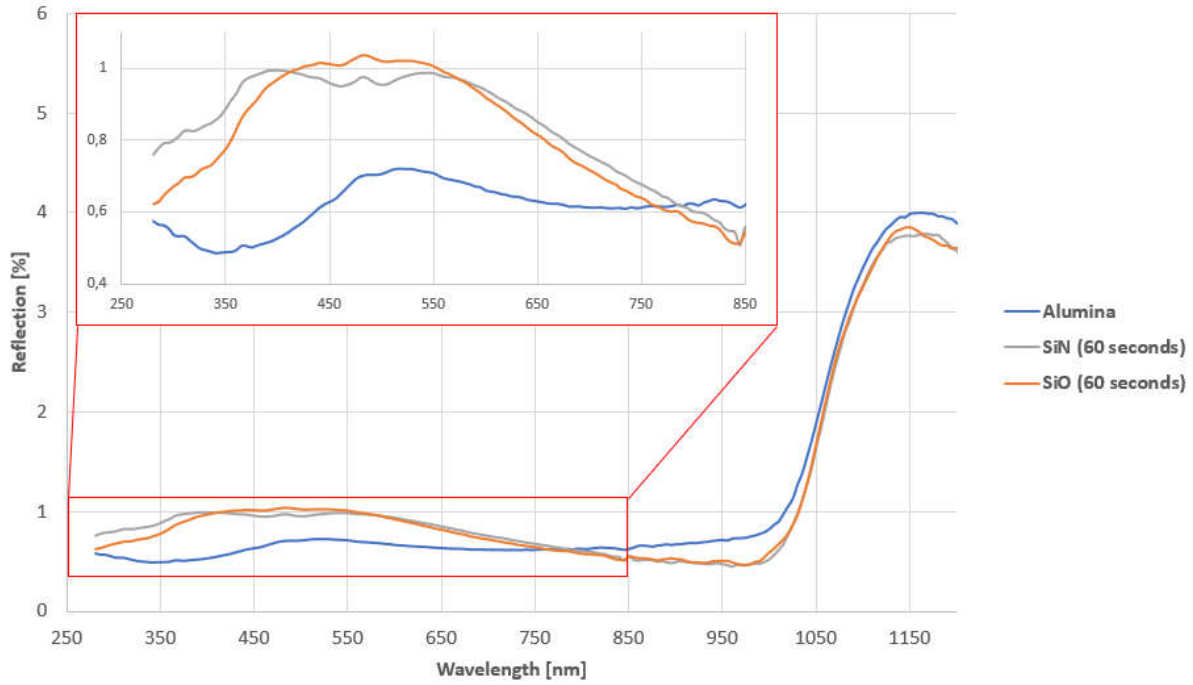

Figure 4.14. Reflection of the samples passivated with alumina, SiO_x (60 seconds) and SiN_y (60 seconds).

The reflection of the alumina passivation layer is kept below 0.8%. When the alumina passivation layer was compared with the two other passivation layers, SiO_x and SiN_y with 60 second deposition time for both, there was an overall lower and more stable reflection for the alumina passivation layer. The low reflection and intact structure show promise for a cheap and easy method for passivating black silicon structures.

4.3 Ag nanoparticles in the alumina

Plasmonic nanoparticles was attempted to be incorporated within the alumina passivation layer. The goal was to deposit the nanoparticles effectively and cost-friendly. The deposition had the same recipe as the chemical alumina passivation layer. Different annealing temperatures were tested, since Ag have a poor wettability. The four temperatures that were investigated was; 450, 600, 750 and 900°C, as illustrated in Figure 3.2. The silver particles were deposited, with varying success, within the passivation layer. All the samples were characterized with surface images and measurements of the reflection.

The sample annealed at 450°C appeared to have small, bright areas that had higher concentration of silver, see Figure 4.15.

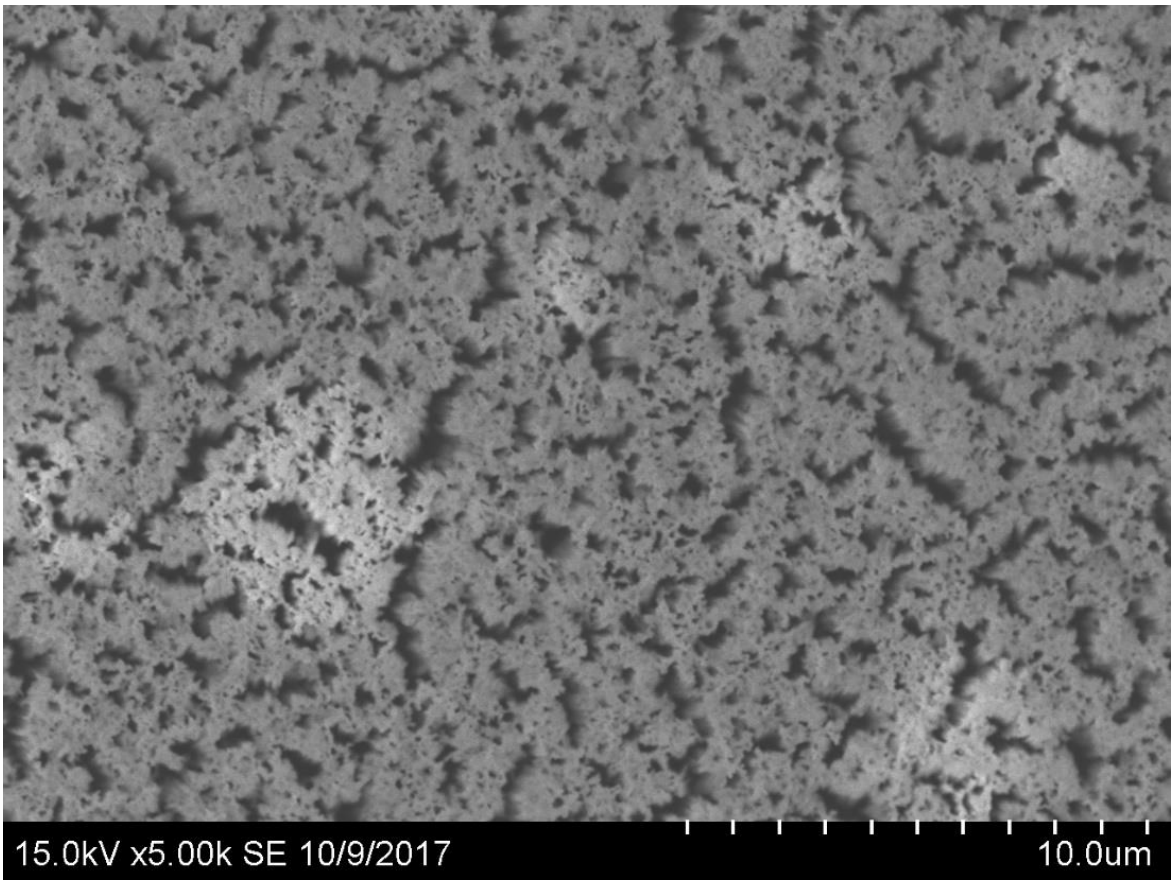

Figure 4.15. Black silicon structure with a passivation layer of alumina with Ag. Deposited wet chemically by dip coating and annealed at 450°C for 3 hours.

The areas had varying diameter, from a 1µm to 6µm. The bright areas were investigated with EDS to confirm the suspicion of higher silver concentration. These areas might be avoided by stirring the solution before deposition and/or have lower heating and cooling rates for the annealing.

The sample that was annealed at 600°C had a good distribution of the particles and the alumina solution. The similar surface nanostructure was kept, see Figure 4.16, with the channels and smaller holes within the channels.

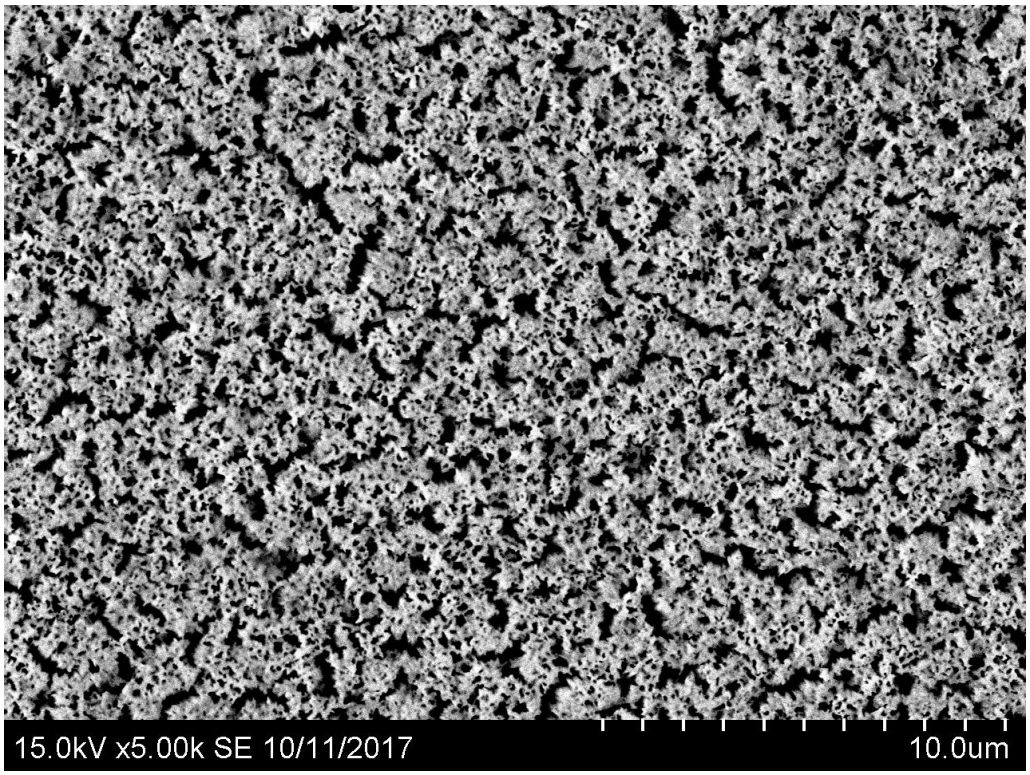

Figure 4.16. Surface of the sample with alumina passivation layer that included Ag nanoparticles, annealed at 600°C for 3 hours. The image has a 5k magnification.

There were no large areas or large particles with silver for the sample annealed at 600°C. Since this surface structure was most promising, this sample were used for further investigation. The cross-section was measured with regards to the thickness. The sample was examined as a powder in S(T)EM and in TEM.

The samples annealed at 750°C and 900°C, had larger silver particles on top of the nanostructure additionally to being spread inside the passivation layer, see Figure 4.17.

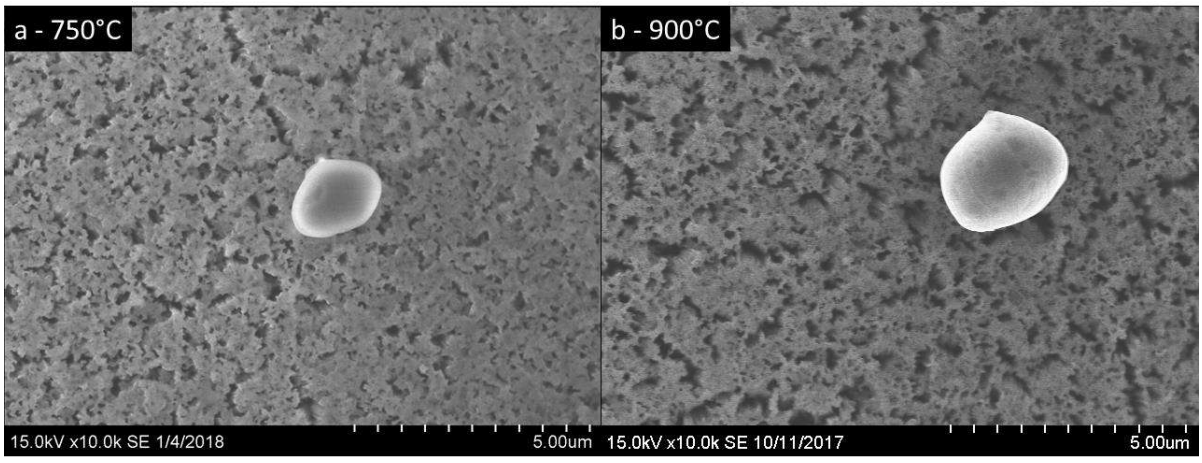

Figure 4.17. Black silicon structure dip coated with solution of alumina and Ag particles and then annealed at 750°C (a) 900°C (b). The large, bright particles was silver, which was confirmed with EDS. Both images were taken with S(T)EM, with 10k magnification.

The measured particles showed that the average particle size for the 900°C sample, compared to the 750°C sample, was bigger. The observed particles had a diameter of approximately 1-3µm. The particles were confirmed being silver with EDS measurements. The temperatures appeared to be a too high temperature for the annealing for the samples annealed at 750 and 900 °C, causing a large silver particle on top of the nanostructure. These particles are too large for a plasmonic effect and should be avoided.

Silver has poor wettability which may be the reason for creating these large particles on top of the nanostructure at high temperatures. Slower heating rate could be beneficial for the samples with the higher silver concentrations. Stirring the solution right before deposition might also lead to improved wettability. A slow heating rate could make it possible for the silver to be homogenously distributed at high temperatures. Different heating/cooling rates should have been tested but were not because of time limitations. The wafers were just dipped and pulled out. A longer holding time for the wafers in the solution, could give other properties. There are several steps to the process that can vary and give variating properties.

The reflection of the samples that had silver nanoparticles and annealed at different temperatures are illustrated in Figure 4.18.

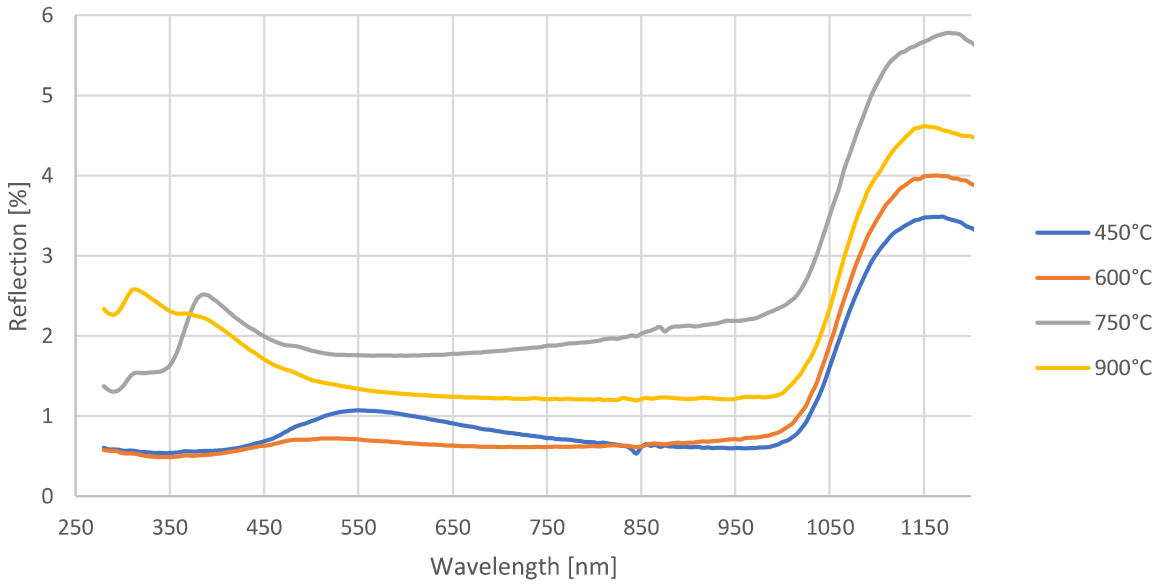

Figure 4.18. Reflection of samples that were chemical passivated with an alumina that included Ag and were annealed at four different temperatures.

The graph shows that the 600°C sample has a stable, low reflection below 1% within the visible light spectrum. The sample that was annealed at 450°C also have low reflection just above 1%, when the light has a wavelength of approximately 550nm. The samples that were

annealed at 750°C and 900°C have more distinguished peaks, around 320nm and 380nm. These peaks will be discussed further in Chapter 4.3.1.3. Even though the optical properties are promising, the black silicon structure must also be kept after deposition of the passivation layer with Ag nanoparticles. The optical and structural characterization shows that the sample annealed at 600°C shows the most promising results and was therefore further examined.

4.3.1 Plasmonic nanoparticles in the alumina passivation layer, annealed at 600°C

The cross-section thickness of the nanostructure was measured for the samples that were passivated with alumina at 600°C, with and without the silver nanoparticles. For comparison, a sample annealed at 450°C and without silver particle was measured. Averages and standard deviations are listed in Table 2, for each of the samples.

Table 2. Different thickness of the nanostructures with and without plasmonic particles at 600°C. And the thickness for the alumina annealed at 450°C without the silver nanoparticles. The table includes the standard deviation for each of the average thicknesses.

Annealing temperature [°C]	Ag nanoparticle	Average thickness [µm]	Standard deviation
450	No	7.61	±0.0788
600	No	7.50	±0.0730
600	Yes	8.72	±0.0756

Both samples without the plasmonic particle has a thickness of about 7.5µm. There is a big difference in the sample with plasmonic nanoparticles, with an average of 8.72µm, which is more than a micrometer thicker. One possible explanation is that the alumina solution changes properties, i.e. viscosity, with the silver nanoparticles. The solution might have had a higher viscosity, resulting in a thicker passivation layer. Again, the nanostructure without the Ag nanoparticles, have become slightly shorter. The same remarks can be done for these samples. The reason may either be mechanical or chemical. There could have been some residue left in the alumina solution after deposition. Since no visual residue were observed, it can be suspected to be a chemical reason for the shorter nanostructure.

4.3.1.1 S(T)EM

When investigating the surface with SEM, there were no evident silver particles found. The images have a scale of micrometers, while the plasmonic particles most likely have a nanometer scale. Therefore, the nanostructure was investigated with EDS at a high magnification of 100k, see Figure 4.19.

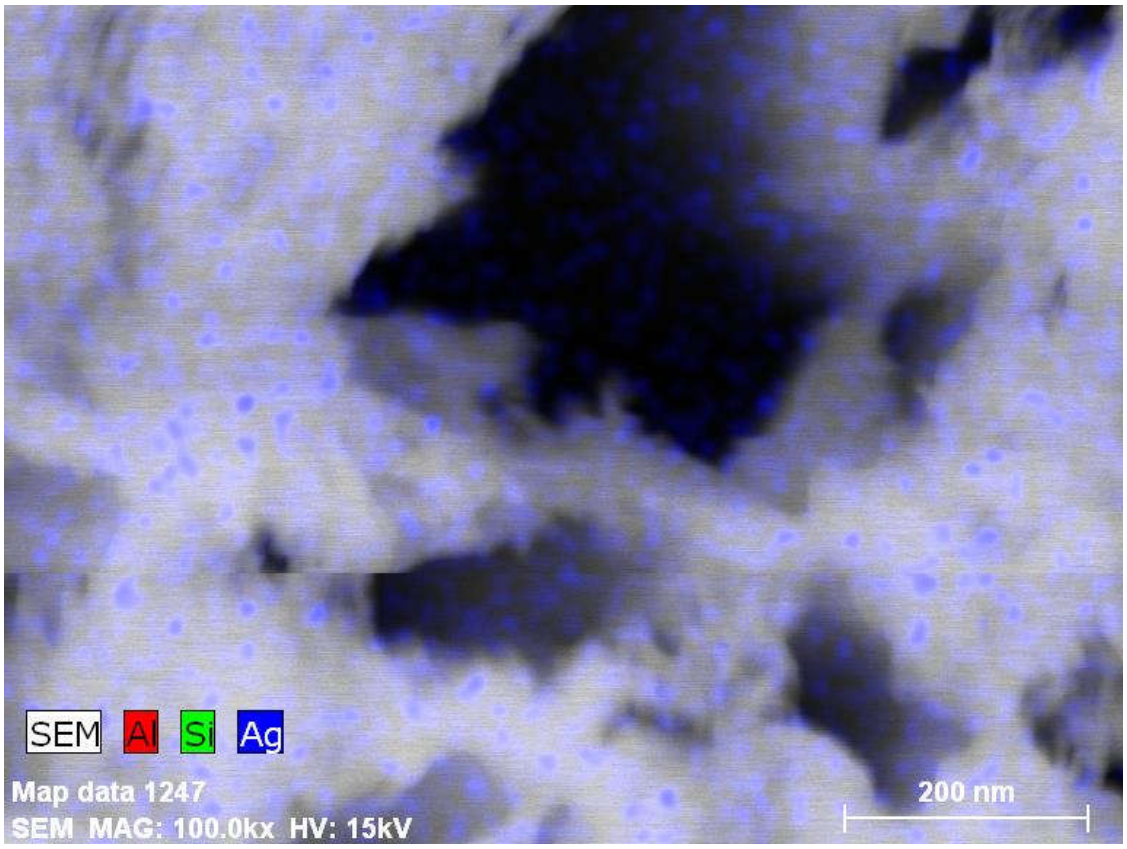

Figure 4.19. EDS image of black silicon structure with a passivation layer of alumina that included Ag nanoparticles. The sample was annealed at 600°C for 3hours. The EDS image have a magnification of 100k. Only the content of silver elements, blue, is illustrated in this image. Detected aluminum and silicon elements have been removed in this image, to illustrate a clearer image of the silver distribution.

It seems that the silver particles have a homogeneous distribution on the surface, in-between the nanostructure. The blue particles are allegedly silver nanoparticles in Figure 4.19, from EDS measurements. If this particle distribution is correct, there are great promise for a good plasmonic effect. The discovered amount of silicon and aluminum have been removed from image 4.19, for a clearer image of the silver distribution. This was an EDS mapping of the structure, which has a large margin of error.

The black silicon structure was scratched of, and used as a “powder”, for investigation with S(T)EM. This approach made it possible to look at individual “nanowires”. The diameter of one single nanowire varied from 100nm to approximately 900nm in diameter. This was a

rough assumption and a large difference gap. The nanowires stick together and made it hard to distinguish each nanowire, see Figure 4.20 as an example.

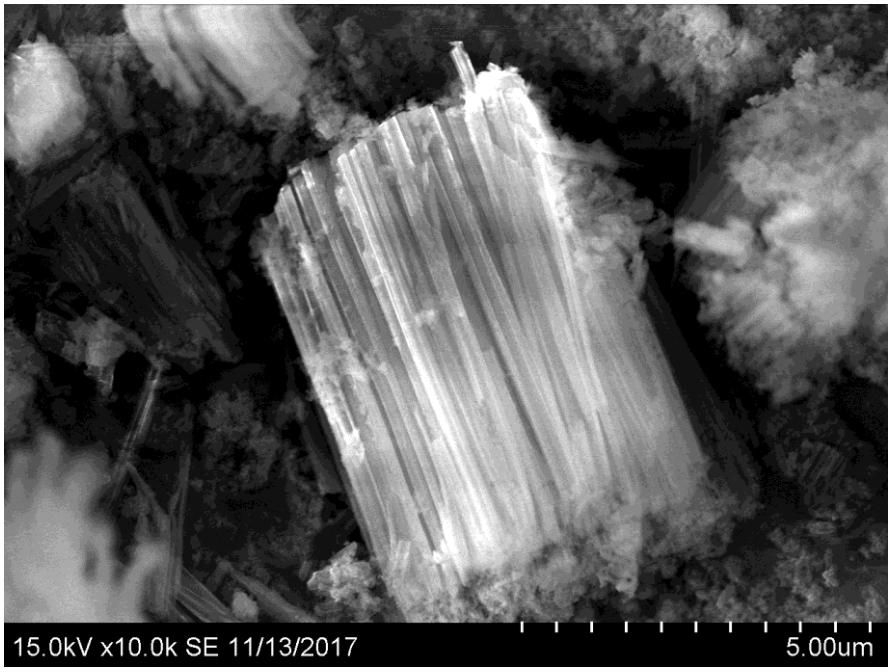

Figure 4.20. When scratching of the nanostructure as a powder, it can be observed bundles of nanowires. This image has a 10k magnification.

The bundle of nanowires that is illustrated in Figure 4.20 was used for EDS measurements. This image and measurements were done with S(T)EM. Where the image has a 10k magnification and the EDS measurements were done at 50k magnification. Figure 4.21 illustrates an element mapping across the bundle of nanowires in Figure 4.20.

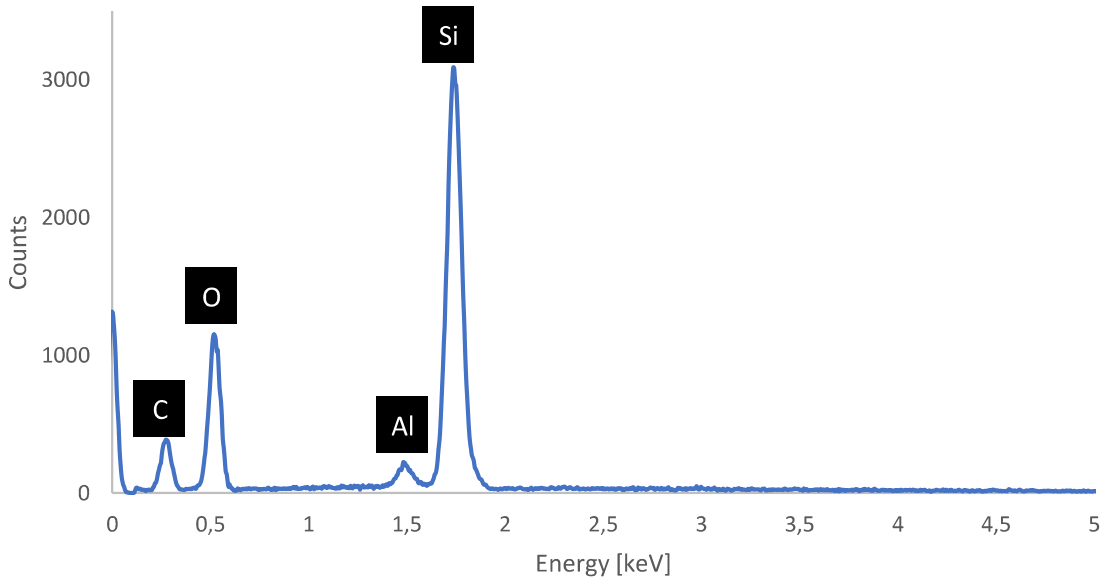

Figure 4.21. EDS line measurements of the bundle silicon nanowires, with 50k magnification

The different peaks were compared to the values that were listed in Table 1; silicon at 1.74keV, aluminum at 1.49keV, oxygen at 0.53keV and carbon at 0.28keV. The peak for aluminum, at 1.49keV, indicates that the passivation layer might have been deposited successfully, but it could also be a disturbance from the sample holder. Oxygen will always be present and therefore have a peak. The carbon peak can have appeared from the carbon tape that have been used, residue or it might be present in the nanostructure. The spectrum shows no indication of silver particles along the line scan. There can be several reasons for this. The areas that were used for the measurements were small and there could simply be no silver at this area. It is also possible that the silver particles were not detected with the line scan. If image 4.19 was correct, some particles should have been detected, since it illustrated a compact distribution of the silver particles. These findings indicate that either Figure 4.19 and/or this EDS line scan, in Figure 4.21, can be misleading results. More information is required, so the powder was also investigated in TEM.

4.3.1.2 TEM

The sample with a passivation layer of alumina that included Ag nanoparticles and annealed at 600°C, was investigated in TEM, as a "powder". Dark areas or particles would indicate heavier elements than in the surrounding areas. Some dark/black particles appeared in the structure in TEM, as in Figure 4.22. These dark particles are attributed to Ag particles forming under annealing.

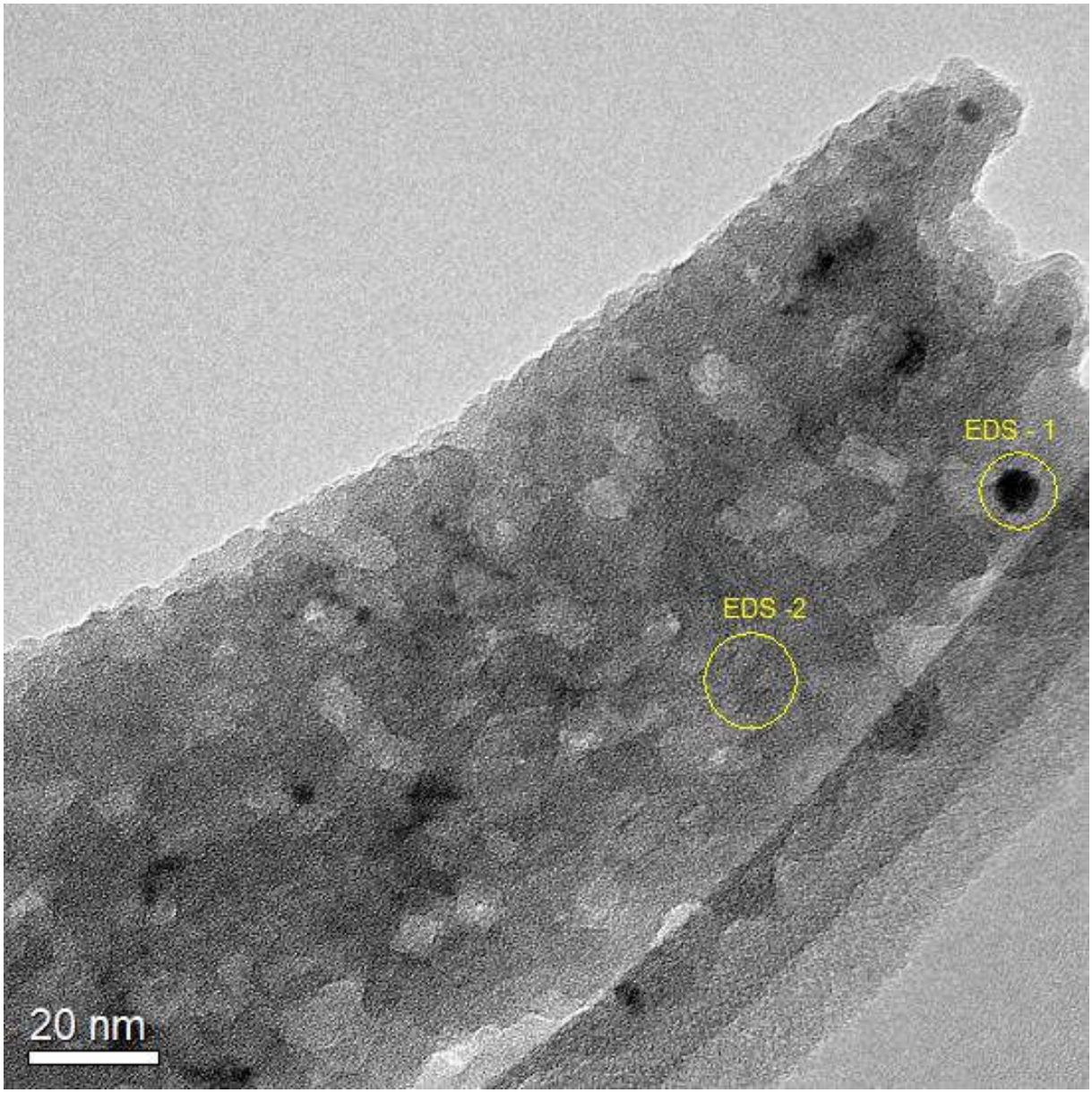

Figure 4.22. TEM image of the black silicon nanostructure, passivated with alumina and Ag nanoparticles. EDS was measured at two points, a dark particle (EDS-1), which was assumed to be silver, and a reference area nearby (EDS-2).

The dark particles had approximately a 10nm diameter. One disadvantage that was observed, is that the nanoparticles appeared to have low distribution over the surface. The shape of the particles was approximately round, which gives a good plasmonic effect. The nanostructure

that was observed in TEM appeared to be very porous, which support the images from 4.10. Where the fracture surface appeared to be brittle and porous.

EDS was used to determine that the dark particle was silver. EDS measurements were done at the dark particle, EDS-1, and at a nearby area, EDS-2, for comparison. Both areas are marked in Figure 4.22, where EDS-1 is marked as the yellow curve and EDS-1 is the blue line in Figure 4.23.

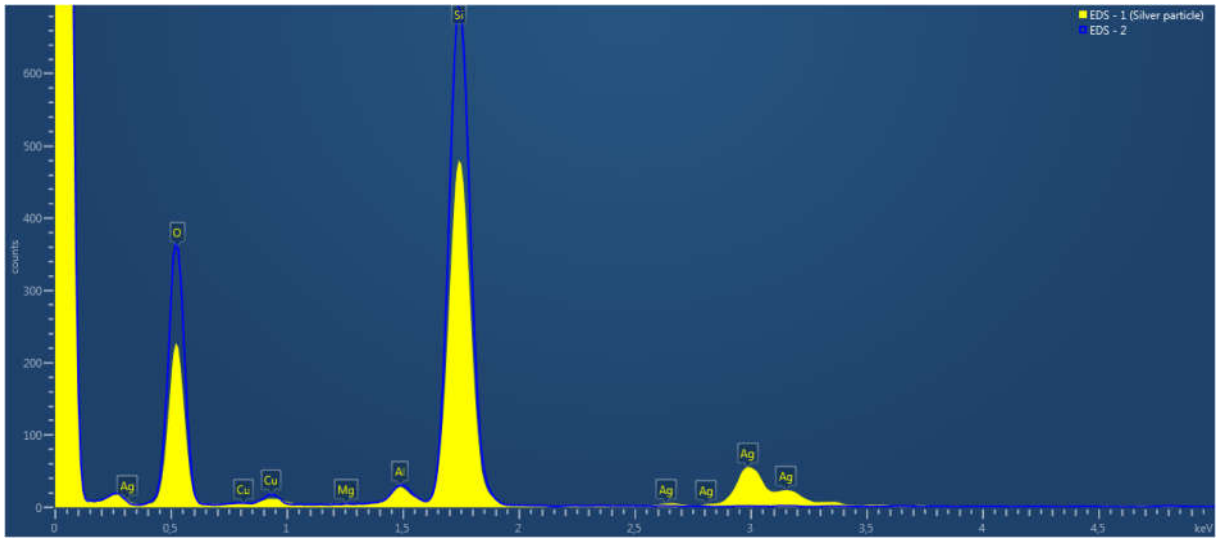

Figure 4.23. EDS measurements of area 1(yellow) and 2(blue) from Figure 4.22.

The EDS spectrum, Figure 4.23, will have some disturbance from the carbon grid, giving Cu peaks. The silicon peaks show a great difference between the two points. There was a lot more silicon in the area where there was no silver nanoparticle and corresponding no silver peaks for the blue line, EDS-2. Silver peaks appears only in the spectrum for EDS-1 or the dark particle, indicating that the dark particle is silver. Area 1 detects the silicon matrix and is therefore a peak in Figure 4.23. Alumina was detected for both measurements, supporting the conclusion that the passivation layer has been deposited successfully.

Bundles of nanostructure were also observed in TEM. Figure 4.24 shows one of these bundles, where it appears to be dark lines, a core, within the structure. It was expected that these lines were the needle-like nanostructure of black silicon structure, created before passivation. The brighter areas around were assumed to be the passivation layer of alumina, a shell. If the chemical deposition of alumina has been successful should there be alumina around the silicon needle-like nanostructure.

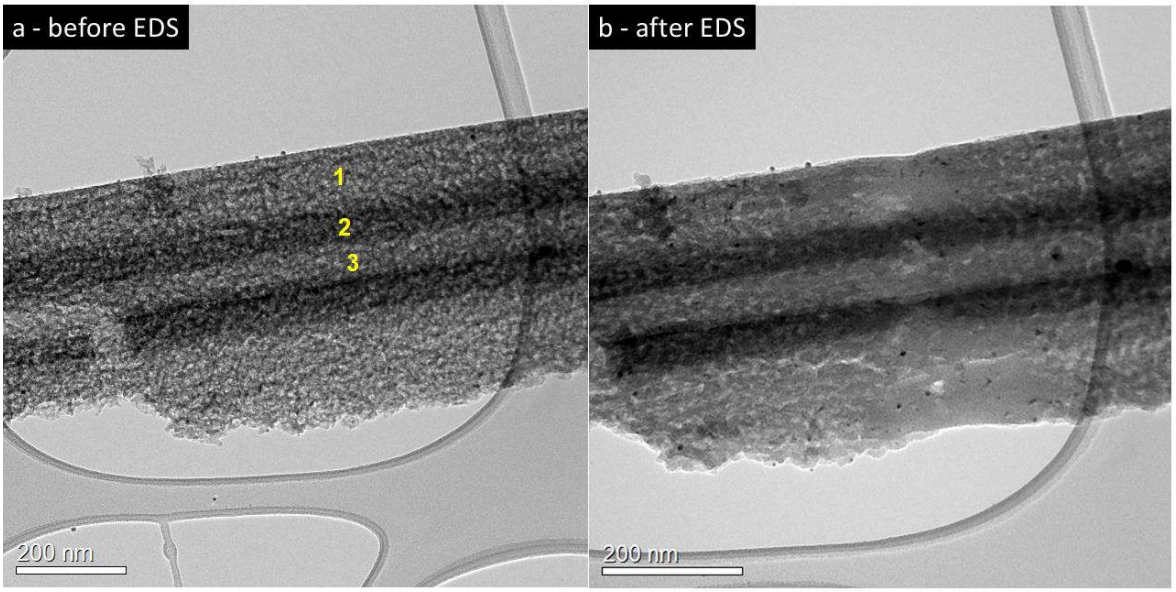

Figure 4.24. TEM image of a bundle of nanowires with alumina passivation layer. Image a *is obtained before the EDS measurements and* b *is after the measurements. The nanostructure has been destroyed, indicating a fragile nanostructure. The three different spots for the EDS measurements are marked with yellow numbers in image* a.

EDS was measured across a bundle of silicon nanowires, as an attempt to determine the different chemical elements between the "core" and the "shell" of the nanostructure. If the passivation layer was successfully deposited, there should have been more silicon in the core and more alumina in the shell around the core. The three different points that were measured are marked in Figure 4.24*a*.

After the EDS measurements, which was done with an accelerating voltage of 200kV, the nanostructure was destroyed. Figure 4.24*b* shows the structure after measurements and show a line across the nanostructure where the detector has measured. This indicate that the nanostructure is fragile. The subsequent measurements were assumed to be misleading and only the three measurements shown in Figure 4.24*a* is used as data for analysis in Figure 4.25. The EDS spectrum from the three points in Figure 4.24*a* shows different chemical composition between the dark area and the brighter outer area. The straight dark lines in the nanostructure was assumed to be silicon nanowires and the bright area could be alumina around the wires.

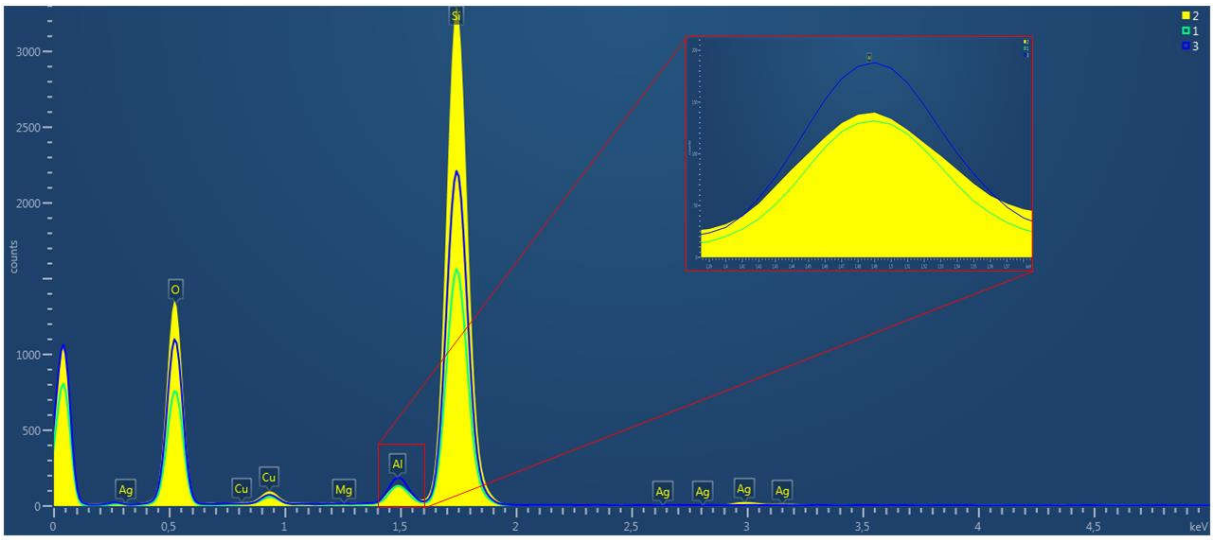

Figure 4.25. EDS of the three different points in image 4.24a. The yellow spectrum is from point 2, the one in the middle, which is assumed to be a nanowire of Si. The green and blue line is points 1 and 3, that are assumed to be the passivation layer around the silicon nanowire.

The EDS spectrum, in Figure 4.25, shows a significant difference between the points. Point 1(green) and 3(blue) have a higher content of aluminum and lower content of silicon, compared to point 2(yellow), enhancing the assumption of silicon nanowires with aluminum passivation layer around the nanowires. The data indicates that the alumina passivation layer have been successfully and homogenously distributed across the nanostructure. There is a difference between point 1 and 3, which is expected to be the same structure of Al. The reason for this can be that the destroyed structure gives some deviations to the three measurements, and then especially for point 3. Since point 3 was between two "cores", this could result in disturbance for the measurements. The spectrum goes only up to 5keV, beyond this, there was some Cu peaks that was assumed to be from the Cu grid.

If these EDS measurements are correct, and the optical properties are acceptable, then there might be useful black silicon nanostructure for application in high efficient solar cells. Some measurements should have been done on the plasmonic effect, to determine if there has been any increase in the overall solar cell efficiency. The fact that silver particles have been deposited successfully within the passivation layer is a big stepping stone for further research. It might be problematic that there is limited control on the size and distribution of nanoparticles, but this might be solved with different concentrations of the chemical solutions. Altered production steps could give different properties.

4.3.1.3 Reflection measurements

The reflection from different samples with and without plasmonic nanoparticles is plotted in Figure 4.26. The figure includes samples with and without the black silicon structures (BSiS).

The four samples with and without BSiS is all passivated chemically with alumina and annealed at 600°C. The final curve, marked as green, is a sample without any surface treatment, a plain and polished monocrystalline wafer.

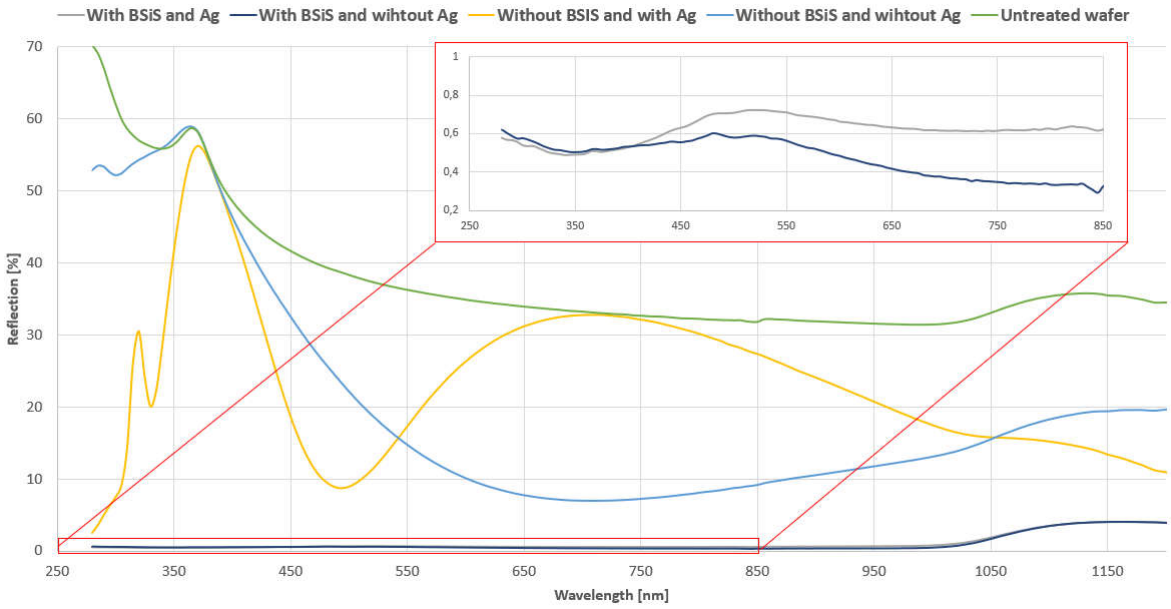

Figure 4.26. Optical graph of the samples with and without the black silicon structure and with and without the Ag nanoparticles, and one untreated wafer.

The untreated wafer (green), sample without the black silicon structure (light blue) and with black silicon structure and Ag particles (yellow) all have a peak around 380nm, in Figure 4.26. It can be assumed that this peak origin from the silicon crystal. The peak is removed for the samples with black silicon structure. Figure 4.26 illustrates that the reflection has been drastically reduced after applying black silicon structure on the surface. The sample that have no black silicon structure and no Ag nanoparticles, but passivated with alumina, is marked as a light blue curve. It can me assumed that alumina works as an anti-reflection coating besides being a passivation layer, since the reflection is reduced after the 380nm, when comparing with the untreated sample (green).

The sample without black silicon structures, with Ag nanoparticles, is marked as the yellow curve in Figure 4.26. It has an approximate shape of cosines to a phase $\varphi = (4\pi nl)/\lambda$, where the n is the refractive index, l is the thickness of the layer and λ is the wavelength. When increasing/decreasing the thickness of the layer, the graph will shift right or left. Silver has a varying refractive index, Equation 10, that gives the "extra" peak around 320nm. It is a large phase change around 350-400nm because of the imaginary and the real part of the refractive index for silver, which is probably causing this peak. These peaks were also observed in

Figure 4.18. Here, the two samples with highest annealing temperatures, 750°C and 900°C, had larger silver particles on top of the nanostructure. These samples had peaks around 320 and 380nm in Figure 4.18, like the yellow curve in Figure 4.26.

Both samples with black silicon, with (grey) and without (dark blue) have both promising low reflection. The samples with the black silicon structure have such a low reflection, that there are no distinguished peaks, compared to the other samples. The magnification of the graph shows that by adding the Ag nanoparticles, the reflection is increased with ~0.2%. This is not a significant change, the reflection is overall low, below 0.8%. These two samples indicate that the good optical properties are kept, even when including the plasmonic nanoparticles.

4.4 Recombination measurements

The lifetime was measured for all the samples with the black silicon structure and passivation layer. The samples were then compared to the reference sample with black silicon wafer without passivation layer and a plain crystalline wafer without any surface treatment. The goal was that the samples got a longer lifetime, and consequently lower recombination in the samples. The measurements would also indicate if the theory is correct, that the recombination is increased after applying the black silicon structure. This would be the case if the wafer had shorter lifetime after application of the black silicon structure, before adding any passivation layer. It could also be interesting to compare the different passivation layer techniques without the black silicon structure. This was not done because of limitations in terms of time.

The µPCD was not able to measure any lifetime for any of the samples, before or after passivation. The device performs contactless measurements and there was no visual damage after the measurements. A plain monocrystalline Si-wafer was measured, but no results were obtained. It can be assumed that it was not possible to measure any lifetime for any of the samples. The samples could have been too small for the instrument, making it hard obtaining accurate measurements. The wafers that was used for all the samples, with and without the black silicon structure, had a very low resistivity of 0.01-0.02Ω cm. This makes the measurements difficult, since the resistance is measured as a function of time. When the resistance is low, it would be difficult for the instrument to measure any lifetime. Equation 7 defined the lifetime, by dividing the excess minority carrier concentration on the recombination rate. µPCD should measure the minority carrier concentration by photoconductance decay to calculating the lifetime and recombination. Samples with low resistivity have a low lifetime, making it difficult to measure.

QSSPC was used on some of the samples, since µPCD gave no results, but it was not possible to measure any lifetime. QSSPC requires larger samples for measurements, therefore only some of the samples were used. The device has contact with the sample, by placing the device on top of the sample, which could damage the surface. Since the measurements gave no results, no lifetime was measured. The same assumptions can be made here, that the resistivity is too low for any detectable lifetime.

There are other factors that can have reduced the lifetime of the sample than the low resistivity. The large surface of a black silicon structure is hard to passivate, giving possibly no effect on decreasing the recombination. There are also possible damages during the annealing step, i.e. contaminations, for the samples with passivation layer of alumina which could have decreased the lifetime. Generally, any contamination can occur during the production steps, which could have a significant influence on lifetime. However, since a reference plain crystalline wafer had no lifetime, no specific conclusions can be done on which options can have influenced the results.

If there is no possibility to measure the lifetime, it is not possible to determine the effect of the passivation layer regarding the electrical properties. Then there is no possibility to determining if the different passivation layer lowered the recombination and increased the lifetime. A conclusion must then be taken with regards to the structure and reflection measurements.

5 Conclusion

The black silicon structure was successfully created with metal-assisted etching, in an ice bath for 20 min. Different passivation layers and methods were tested. Silicon oxide and silicon nitride were passivated with PECVD, with variating deposition times. A chemical deposition method was also tested with alumina. Plasmonic silver particles were included in an alumina passivation layer with the purpose of a plasmonic effect.

- A passivation layer of silicon oxide, with PECVD, was deposited on different samples with black silicon structure with varying deposition times.
    - The optical and surface structural results indicated a successful deposition of the passivation layer.
    - The cross-section showed that the shortest, 15 seconds, and longest, 60 seconds, deposition time had the best nanostructure. This result was most likely caused by poor sample preparation for the intermediate deposition times (30 and 45 seconds).
- A passivation layer of silicon nitride, with PECVD, was deposited on different samples with black silicon structure with varying deposition times.
    - The shortest deposition times, 15 and 30 seconds, had most promising results, regarding the low reflection and the intact structure after passivation.
    - The sample with 45 second deposition time had a good surface structure, but slightly higher reflection and the cross-section showed a brittle nanostructure.
    - The surface structure of the sample with 60 seconds deposition time was destroyed after deposition. The reflection was also high, compared to the other three samples.
- A passivation layer of alumina was successfully wet chemically deposited, with annealing temperature of 600°C for 3hours.
    - The surface and cross-section structure were kept after passivation.
    - The sample had great optical properties, with low reflection, under 0.8%, within the visible light spectrum.
- Plasmonic nanoparticles were successfully incorporated into the alumina passivation layer.
    - From the four different annealing temperatures that were tested, 600°C was the most successful. An annealing temperature of 450°C created large areas with high concentration of silver on the surface. The samples with annealing temperatures of 750°C and 900°C had larger silver particles on top of the nanostructure.
    - The reflection measurements showed distinguished peaks from the silver particles.

    - TEM was used for the sample with annealing temperature of 600°C, to verify that the silver particles were successfully deposited within the passivation layer. Average diameter of the silver nanoparticles was approximately 10nm.
    - More measurements are required regarding the plasmonic effect.
- Measurements of the lifetime gave no valid results.
    - The lack of results was assumed to be due to low resistivity in the wafers that were used.
    - There was no possibility to determine if the recombination have been increased/decreased after deposition of the different passivation layers, since the lifetime was not measured.

The results from incorporating the Ag plasmonic nanoparticles within the alumina passivation layer has great promise for high efficient solar cell. The production steps are cheap and easy to use at a large industrial scale. Grid parity could be achieved, if the recombination is reduced with the alumina passivation layer and the Ag nanoparticles have a plasmonic effect.

References

1. Liu, X., et al., *Black silicon: fabrication methods, properties and solar energy applications.* The Royal Society of Chemistry, 2014.
2. Juul, M.E., *Black Silicon Solar Cell Structures*, in *Department of Materials Science and Engineering*. 2016, Norwegian University of Science and Technology.
3. Aberle, A.G. and U.o.N.S.W.C.f.P. Engineering, *Crystalline Silicon Solar Cells: Advanced Surface Passivation and Analysis*. 1999: Centre for Photovoltaic Engineering, University of New South Wales.
4. Catchpole, K.R. and A. Polman, *Plasmonic solar cells.* Optics Express, 2008. **16**(26): p. 21793-21800.
5. Maier, S.A., *Plasmonics: Fundamentals and Applications : Fundamentals and Applications*. 2007, Boston: Boston, MA, US: Springer US.
6. Garnett, E. and P. Yang, *Light Trapping in Silicon Nanowire Solar Cells.* Nano Letters, 2010. **10**(3): p. 1082-1087.
7. Oates, T.W.H., H. Wormeester, and H. Arwin, *Characterization of plasmonic effects in thin films and metamaterials using spectroscopic ellipsometry.* Progress in Surface Science, 2011. **86**(11): p. 328-376.
8. Nelson, J., *The physics of solar cells*. 2003, London: Imperial College Press.
9. Callister, W.D. and D.G. Rethwisch, *Material Science and Engineering*. 8th ed. ed. 2011: Wiley.
10. Lehmann, V., *Electrochemistry in Silicon: instrumentation, science materials and applications*. 2002, Weinheim: Wiley-VCH Verlag.
11. Dingemans, G. and W.M.M. Kessels, *Status and prospects of Al2O3-based surface passivation schemes for silicon solar cells.* Journal of Vacuum Science & Technology A: Vacuum, Surfaces, and Films, 2012. **30**(4): p. 040802.
12. Albadri, A.M., *Characterization of Al2O3 surface passivation of silicon solar cells.* Thin Solid Films, 2014. **562**: p. 451-455.
13. Pawlik, M., et al., *Electrical and Chemical Studies on Al2O3 Passivation Activation Process.* Energy Procedia, 2014. **60**: p. 85-89.
14. Rahman, M.Z. and S.I. Khan, *Advances in surface passivation of c-Si solar cells.* Materials for Renewable and Sustainable Energy, 2012. **1**(1): p. 1.
15. Liu, B., et al., *Silicon Nitride Film by Inline PECVD for Black Silicon Solar Cells.* International Journal of Photoenergy, 2012. **2012**: p. 5.
16. Grant, N. and K. McIntosh, *SURFACE PASSIVATION ATTAINED BY SILICON DIOXIDE GROWN AT LOW TEMPERATURE IN NITRIC ACID*. 2017.
17. Aberle, A.G., *Overview on SiN surface passivation of crystalline silicon solar cells.* Solar Energy Materials and Solar Cells, 2001. **65**(1): p. 239-248.
18. Aberle, A.G., *Surface passivation of crystalline silicon solar cells: a review.* Progress in Photovoltaics: Research and Applications, 2000. **8**(5): p. 473-487.
19. George, S.M., *Atomic Layer Deposition: An Overview.* Chemical Reviews, 2010. **110**(1): p. 111-131.
20. Wolf, S.D. and G. Beaucarne, *Surface passivation properties of boron-doped plasma-enhanced chemical vapor deposited hydrogenated amorphous silicon films on p-type crystalline Si substrates.* Applied Physics Letters, 2006. **88**(2): p. 022104.
21. Horányi, T.S., T. Pavelka, and P. Tüttö, *In situ bulk lifetime measurement on silicon with a chemically passivated surface.* Applied Surface Science, 1993. **63**(1): p. 306-311.
22. Fu, Q., C.-B. Cao, and H.-S. Zhu, *Preparation of alumina films from a new sol–gel route.* Thin Solid Films, 1999. **348**(1): p. 99-102.

23. Jain, P.K., et al., *Review of Some Interesting Surface Plasmon Resonance-enhanced Properties of Noble Metal Nanoparticles and Their Applications to Biosystems.* Plasmonics, 2007. **2**(3): p. 107-118.
24. Streetmann, B. and S.K. Banerjee, *Solid State Electronic Devices*. 6th edition ed. Prentice Hall series in solid state physical electronica, ed. N. Holonyak. 2006, Upper Saddle River, NJ: Pearson.